Energy & Buildings 333 (2025) 115416

Contents lists available at ScienceDirect

Energy & Buildings

journal homepage: www.elsevier.com/locate/enb

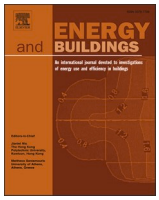

From energy-intensive buildings to NetPlus targets: An innovative solar exoskeleton for the energy retrofitting of existing buildings☆

Roberto Stasi *, Francesco Ruggiero, Umberto Berardi

Department of Architecture, Built Environment and Design, Polytechnic University of Bari, Bari, Italy

ARTICLE INFO

Keywords:
ZEB
Mediterranean climate
Exoskeleton
Building energy retrofitting
Existing buildings
BEM
RES integration

ABSTRACT

The retrofitting of existing buildings is a challenging strategic objective towards achieving the European climate neutrality target by 2050. According to the Renovation Wave plan, the European Union aims to renovate around 35 million existing inefficient buildings to the highest energy efficiency level by 2030, requiring innovative technological solutions to succeed in this ambitious goal. Along this line, this paper proposes a prototype of a novel solar exoskeleton for the energy and architectural retrofitting of existing buildings, called "en-SOLEX". The system comprises a self-supporting external steel frame that envelops buildings like a double skin. It combines passive solar gain control, such as shading and greening, with high-efficiency active solar systems, including PV panels. The system's modular and flexible design makes it easy to install, allowing for retrofitting from the outside without affecting occupancy, reducing the time and cost of its implementation. The energy-saving potential of the system, thermal and daylight comfort, and payback period with different façade configurations were evaluated on a multi-family residential building in a Mediterranean climate. The energy simulations demonstrate that the proposed solution can significantly reduce the energy required for space heating and cooling, by 33.4% and 25.5% respectively. A maximum reduction of 80.7% and 60.5% for heating and cooling is achieved by integrating the "en-SOLEX" system with generator replacement. The integration of renewable energy sources leads to surplus electricity generation, which causes the building to exceed its average annual electricity demand regardless of the building orientation, thus transforming the existing building into a NetPlus one.

1. Introduction

For several decades, the European Commission has been pursuing the objectives of reducing energy consumption and increasing energy efficiency in the building sector. The European Green Deal has set new targets for the transition from fossil fuels to renewable energy, to achieve climate neutrality by 2050 [1]. The European Union has recently adopted the "Fit for 55" package to implement the Green Deal Act, which aims to reduce net greenhouse gas emissions by 55 % by 2030 compared to 1990 levels. It is important to note that the EU only managed to decrease its emissions by 20 % between 1990 and 2020, highlighting the magnitude of the action needed to reach this goal. Therefore, a comprehensive energy transition plan involving all sectors of European society is necessary to achieve this ambitious target in less than a decade [2].

The building sector has always been identified as one of the most energy-intensive, but it is also the sector where energy efficiency targets are most easily achievable and cost-effective [3]. Buildings are responsible for approximately 40 % of the EU's final energy consumption and 36 % of its carbon dioxide emissions [4]. The residential sector alone accounts for 26.1 % of final energy consumption and 16.6 % of gross inland energy consumption [5]. These significant shares emphasize the reasons why European energy policy is increasingly focusing on efficiency measures in the building sector [6]. In this sense, the Energy Performance of Buildings Directive (EPBD) introduced in 2010 the obligation to build only nearly Zero Energy Buildings (nZEB) from 2021 onward [7].

While the number of nZEBs is increasing across Europe [8], they are primarily limited to new constructions and represent only a small portion of the overall European building stock. Therefore, in 2018, the recast of the European Directive 844/2018 [9], placed particular stress on the energy renovation of existing buildings, which make up the largest share in Europe. The latest draft of the EPDB revision, updated following the "Fit for 55" package, further emphasizes the importance of improving the energy efficiency of existing buildings as a key objective

☆ This article is part of a special issue entitled: 'Housing energy transition' published in Energy & Buildings.

* Corresponding author.
E-mail address: roberto.stasi@poliba.it (R. Stasi).

https://doi.org/10.1016/j.enbuild.2025.115416
Received 3 April 2024; Received in revised form 8 January 2025; Accepted 31 January 2025
Available online 12 February 2025

Nomenclature

BIPV	building integrated photovoltaic
COP	coefficient of performance
CV(RMSE)	coefficient of variation
D	daylight factor
EER	energy efficiency ratio
EPBD	Energy Performance of Buildings Directive
EU	European Union
HP	heat pump
M	measured data
MBE	mean bias error
nZEB	nearly zero energy building
PBP	payback period
PV	photovoltaic
RC	renewable energy coverage
RES	renewable energy source
RMSE	root mean square error
S	simulated data

Symbology

$d(t)$	delivered electricity
$e(t)$	exported electricity
$g(t)$	electricity generation
$ne(t)$	net electricity
$s(t)$	self-consumed electricity
T_{mr}	mean radiant temperature
T_{op}	operative temperature
λ	thermal conductivity
D_T	reference daylight factor
D_{TM}	minimum reference daylight factor

for an effective energy transition in the European Union.

Indeed, a significant quota of the building stock in Europe is more than 50 years old and has been identified as inefficient, requiring the significant implementation of retrofit measures to reduce energy demand and CO_2 emissions [10]. For instance, in Italy, about 86 % of the existing building stock was built before 1991 [11], when the first regulation that effectively promoted energy efficiency in the building sector came into force. As a result, the majority of the Italian building stock has significant energy efficiency shortages and needs to be significantly renovated, given the European targets for decarbonisation of the building sector [12]. In line with the European Green Deal, the EU has developed a "renovation" strategy and action plan, which includes specific measures to increase renovation activities. According to the Renovation Wave plan, around 35 million existing buildings need to be upgraded to the highest energy efficiency level by 2030, and innovative technological solutions are required to achieve this ambitious goal [13].

While achieving nearly zero energy targets for new buildings is relatively easy, upgrading existing buildings to meet these standards is much more complex [14]. Decreasing energy consumption in existing buildings is, in fact, a costly process. This is due to the higher density of the consolidated urban context, the inherently energy-intensive nature of existing buildings, and the considerable heat dispersion of the building envelope [3,15,16]. Furthermore, integrating renewable energy sources (RES) into existing buildings may not effectively cover the overall building energy demand due to limited available surfaces and poor structural load-bearing capacity, particularly in high-density urban areas [17,18].

Several studies focused on the energy refurbishment of existing buildings to improve their energy performance [19–25]. One primary method for developing low-carbon buildings is to upgrade the thermal efficiency of the building envelope components passively [26]. This can be achieved by adding additional layers of thermal insulation to opaque envelope surfaces [23,27] or replacing existing windows with double or triple-glazing systems to reduce heat loss through envelope surfaces and thermal bridges [28].

Passive retrofitting is recognised as essential for the development of low-carbon buildings. By improving the thermal transmittance of the building envelope, depending on climatic zones, it is possible to achieve heating energy savings of up to 58.3 % [29]. Additionally, the integration of innovative materials, such as Phase Change Materials (PCMs), in existing building envelopes can further increase the total annual energy saving [30]. Along this line, research by Dardouri et al. [31] demonstrated that integrating PCMs with 6-cm-thick EPS insulation panels led to a notable enhancement in the energy-saving performance of the insulation, increasing from 26.9 % to 46.3 %, thereby improving the building's thermal behaviour even during the cooling period.

When implementing these strategies, especially in hot climates, it is crucial to address the issue of overheating during cooling months [32,33]. Enhancing hybrid or natural ventilation within the building during the cooling period has been proven to be effective in reducing overheating issues caused by over-insulation of the external envelope [34–37]. Even the addition of a fixed or shading system can significantly reduce the overheating risk reducing energy demand for cooling and improving thermal comfort [38–40]. Such renovation strategies primarily focus on curbing the building's energy consumption, neglecting the critical need to significantly enhance on-site energy generation to meet the majority of the building's energy demand [41].

To address this issue, an even more effective solution is the use of active retrofitting measures combined with the integration of renewable energy sources. The retrofitting of existing heat generation with a combined use of heat pumps and photovoltaic (PV) systems, is considered the most cost-effective solution to cover existing building demand and reduce grid energy load [42,43].

In the context of retrofitting energy in residential buildings, the most commonly employed actions include external wall insulation, the replacement of obsolete plant systems and the integration of PV technology. Ballarini et al. [44] evaluated the most effective energy efficiency measures and found that replacing both envelope components and heat generators produces an average of 65 % energy savings. Along the same line, Calise et al. [45] demonstrated that the integrated use of a heat pump, thermal insulation, and a photovoltaic field, with a lithium-ion battery resulted in a 52 % reduction in primary energy consumption and a 49 % reduction in CO_2 emissions, increasing the self-consumed electricity of existing retrofitted building.

Nevertheless, the integration of renewable energy into existing buildings often requires a large area to meet the building's energy needs. Therefore, most measures for integrating photovoltaics only focus on the available roof surface, which is usually insufficient, especially for high-rise buildings. For this reason, new solutions involving building integrated photovoltaics (BIPV) are becoming increasingly popular [46–48]. Xiang et al. [49] evaluated the energy performance of a novel BIPV system. The study discovered that PV panels of varying colours can cover up to 62.3 % of the annual household energy consumption for a high-rise building in Norway.

Recent research tries to offer holistic solutions to the retrofitting of existing buildings aiming to improve both their energy and seismic performance [50,51]. Along this line, Evola et al. [52] investigated the energy performance of a prefabricated timber-based retrofit solution which allows reducing the energy need for space heating and space cooling by 66 % and 25 %, respectively.

Santarsiero et al. [53] proposed an RC exoskeleton equipped with insulation panels for the retrofit of a school building. The suggested

reinforced concrete (RC) exoskeleton, incorporating insulation panels, led to a notable enhancement in the seismic capacity-demand ratio, increasing it by a factor of five. Simultaneously, thanks to PV integration on the roof and heat generator replacement, the total non-renewable energy consumption was reduced by approximately 80 %.

Nevertheless, these solutions are hardly able to provide net zero goals in existing residential building renovation. Thus, a promising innovative solution is spreading the use of steel exoskeletons for the energy retrofitting of existing buildings [54–56]. The use of steel exoskeletons is a technological solution for enhancing building facade performance, reducing building energy demand, and increasing building structural capacity [57]. The exoskeleton acts as an external framework, enveloping the existing buildings either partially or entirely, creating usually discrete connections at specific points with the existing building structure. This addition enhances the strength and rigidity of the existing structure even against seismic forces, while also creating a new external envelope configuration, such as integrated double-skin or ventilated façade designs [58]. The exoskeleton envelope can be positioned both against the building or set apart from the existing façade to create additional living spaces, balconies, solar greenhouses and buffer zones improving thermal comfort and liveability.

Steel exoskeletons may have significant implications for sustainability and environmental performance, in addition to their structural and architectural benefits. These external frameworks can improve energy efficiency and reduce energy demands in the retrofitted building, contributing to the overall sustainability of the built environment [59,60]. The use of renewable energy technologies, such as photovoltaic panels and solar shading devices, can improve the energy performance of buildings. Furthermore, despite steel representing a material with greater embodied energy, around 32–35 MJ/kg [61], the lightweight nature of steel construction and its high structural strength per square meter compared to other construction materials reduces the carbon footprint associated with transportation and installation [62]. When comparing the embodied energy of potential exoskeleton materials, such as steel, aluminum, and structural timber, steel exhibits a higher embodied energy than timber but a lower energy demand compared to aluminum production. Conversely, when considering the entire LCA assessment of the material from cradle to cradle, the high percentage of recycled content in steel and the ability to be recycled multiple times without significant degradation in quality reinforce its sustainability profile, positioning it as a viable solution compared to traditional building materials such as reinforced concrete and structural timber

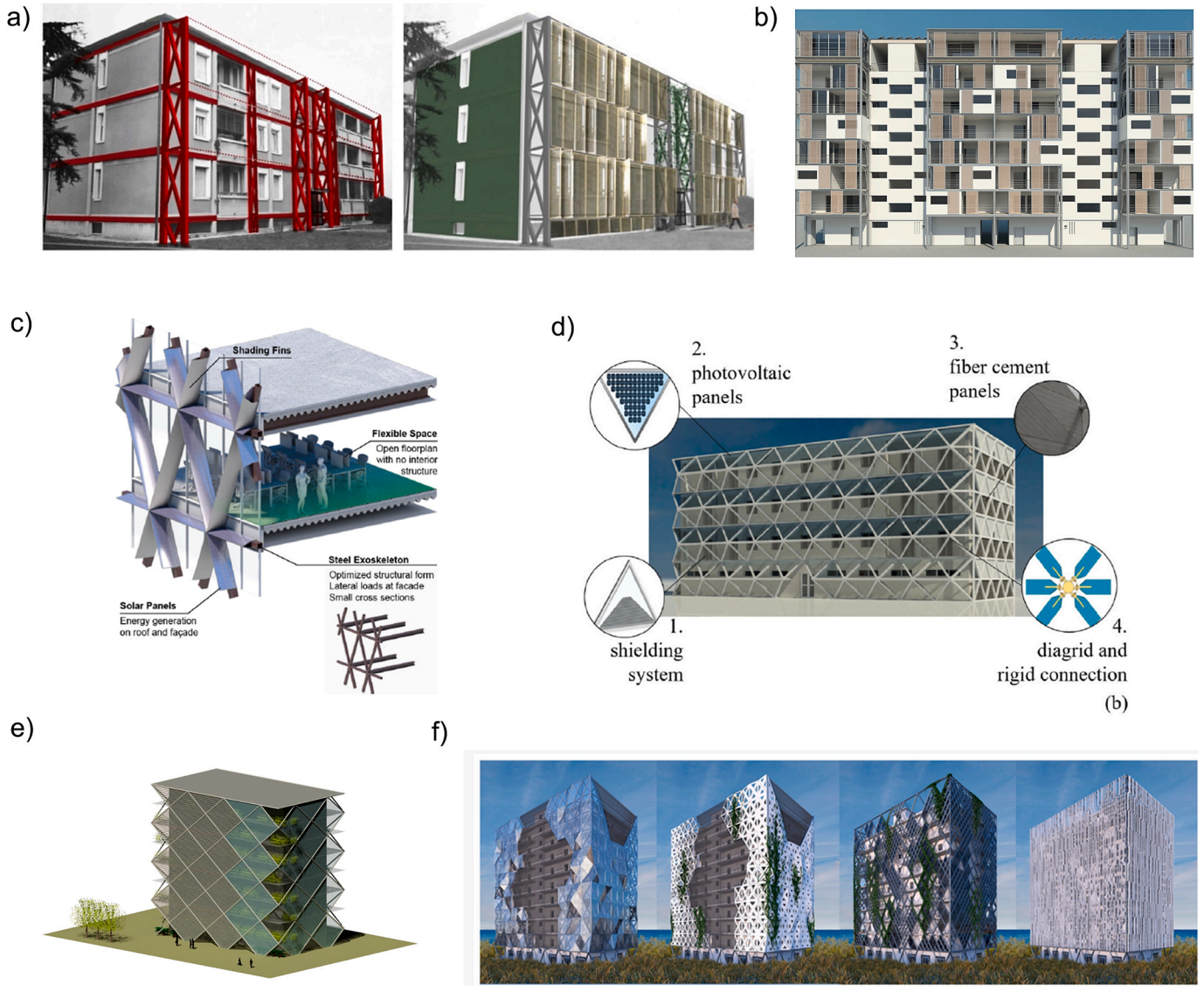

Fig. 1. Exoskeleton for reinforced concrete buildings: a) Marini et al. [62], b) Ferrante et al. [66], c) Weber et al. [60], d) D'Agostino et al. [18], e) Labò et al. [56] and f) D'Urso et al. [67].

where glues and preservatives combined with the natural degradation of the material may make it difficult to reuse and recycle [63,64].

Another benefit of these solutions is that they primarily require intervention from outside the building, minimizing the need for renovations and optimizing implementation time and costs without causing interference from occupants.

Despite their many benefits, steel exoskeletons also present challenges and considerations that must be addressed during the design and implementation process. Factors such as material selection, structural detailing and compatibility with the existing building must be carefully evaluated to ensure optimal performance and longevity [55]. In addition, the cost implications of incorporating steel exoskeletons into building projects can be a barrier to widespread adoption, requiring a thorough cost-benefit analysis to justify the investment.

Bellini et al. [65] proposed a combining seismic retrofit with energy refurbishment for the sustainable renovation of reinforced concrete buildings. The steel exoskeleton system which features solar greenhouses on the southern façade, along with thermal insulation using EPS, new energy-efficient windows, and adjustable louvre shading systems for controlling solar radiation can ensure a 70 % reduction in heating energy consumption of a retrofitted building (Fig. 1a).

Along the same line, Ferrante et al. [66] developed a multifunctional steel exoskeleton within the Pro-GET-onE project. This exoskeleton integrates various technologies to create thermal buffer zones, such as balconies or additional space, which help to reduce solar radiation during the summer months, provide solar heating during the winter, and support plug-and-play installations for new HVAC systems (Fig. 1b). Additionally, the exoskeleton integrates photovoltaic (PV) panels on the roof. The system can reduce energy consumption by up to 75 % during the winter months, with overall reductions of 35 % reported based on simulations conducted for three case study locations (Greece, Italy and Romania).

An alternative integrated exoskeleton system can be implemented by using diagonal grids, or "diagrids," as exoskeletons. These grids incorporate façade elements directly, offering structural, energy, and architectural enhancements. Weber et al. [60] designed a diagrid steel exoskeleton for mid-rise and high-rise new buildings. The system can reduce embodied and operational carbon by 37–80 % and 24–48 %, respectively. In addition, the diagrid system equipped with PV panels can achieve a net zero target with on-site production exceeding 134 % to 127 % of the building energy needs depending on building heights (Fig. 1c).

A diagrid exoskeleton with PV panels for the energy and seismic retrofit of existing buildings was proposed by D'Agostino et al. [18]. The system can cover 47.5 % to 54 % of building electricity demand by PV on-site generation using PV panels integrated into windows (Fig. 1d).

Labò et al. [56] presented an optimised design approach for the diagrid system (Fig. 1e). This approach was aimed at minimising the impacts and costs of the intervention throughout the life cycle of the building. Similarly, a parametric optimisation algorithm was employed by D'Urso et al. [67] to identify the most material-efficient diagrid exoskeleton (Fig. 1f). Subsequently, several design concepts for integrated retrofitting were developed, including renewable energy generation options such as building-integrated photovoltaics (BIPVs), vertical gardens or "green walls" that enhance passive cooling, and solar shading devices, such as louvre systems, to regulate solar radiation and natural lighting. However, this study focused on the structural optimisation analysis of the steel system without providing information about the potential energy savings produced by the system. Although diagrid systems allow for greater flexibility and ease of structural integration with the existing building and require less available space for their use, these systems are more complex to design, necessitating the implementation of tailored solutions. Furthermore, due to the nature of their structure and their spatial layout, they do not facilitate straightforward integration of renewable sources or reduce their efficiency.

With recent advancements in district and community-level strategies, exemplified by the emergence of concepts such as Positive Energy Districts (PEDs), there is an increasing need for deep renovation within the residential building sector. Therefore, to significantly improve the energy performance and efficiency of existing buildings, innovative strategies are essential. Such interventions have the potential to transform retrofitted residential buildings into postive energy producers at the district level [68,69].

This paper proposes an innovative solution: a solar exoskeleton designed for both energy optimization and architectural retrofitting of existing buildings, called "en-SOLEX". The system comprises a steel exoskeleton that incorporates passive energy-saving strategies, including shading and insulation, with high-efficiency active solar technologies, such as photovoltaic panels. By integrating the system into existing buildings, the aim is to provide an innovative and flexible solution for architects and public organizations to transition from energy-intensive to net-positive energy buildings.

2. The "en-SOLEX" system

The en-SOLEX system is a stand-alone self-supporting steel frame exoskeleton that is applied directly to the exterior of an existing building to improve its energy performance. The system aims to increase the available surface area for the integration of RES in existing medium and high-rise buildings, which is particularly important as these buildings often have limited space available for solar panels, typically limited to the roof surface. The exoskeleton's metal structure is designed as a simple steel frame composed of beams and pillars connected by plates using screws and bolts. This design choice was made to reduce both the cost and complexity of the intervention when compared to diagrid exoskeleton systems.

The EN-SOLEX system has been mainly developed for implementation in apartment blocks; its primary focus of application is on post-Second World War reinforced concrete structures, which account for approximately 50 % of the European building stock [70]. These buildings, frequently found in deteriorating urban suburbs, are typically multi-storey frame structures isolated from neighbouring buildings. They are characterized by poor and undistinguished architectural features, high operational energy demands, low living comfort, and significant seismic vulnerability.

This building typology is chosen for the development of the system based on the typological archetypes analysis from the existing Italian building stock according to the TABULA project [71,72]. The TABULA project identified several national building typologies classes within the existing European building stock based on a set of model residential buildings that reflect common morphological and energy characteristics. Among the studied classes, the class 6, which includes multi-family buildings built between 1976 and 1990, was selected.

This building typology class is typically characterised by a rectangular floor plan, with the longer sides between 15 and 24 m and the shorter sides between 8 and 12 m, usually shared with adjacent building units. Such buildings tend to have similar geometric and structural characteristics, consisting of a central staircase and two apartments of varying sizes per floor. Geometrically, they are often characterised by a linear external profile and a modular structural grid. Given a floor height of 2.7 m for the housing spaces [73], based on the typical inter-storey between reinforced concrete beams of the typological existing building structural frame and the typical building plan length, the steel frame exoskeleton operates on a modular grid of 3 m x 3 m, constructed using 200 mm H-section pillars and 140 mm I-section beams (Fig. 2). It comprises two primary elements: a frame aligned parallel to the building's façade, functioning as an anchoring mechanism, and an outer façade tilted at a 5° angle from the vertical axis, aimed at enhancing the solar absorption capabilities of the integrated photovoltaic systems. The tilt of the secondary structure with respect to the vertical was limited to 5° to minimise the space required for the system integration at the ground floor, as the height of the building varies (up to 3 m considering a

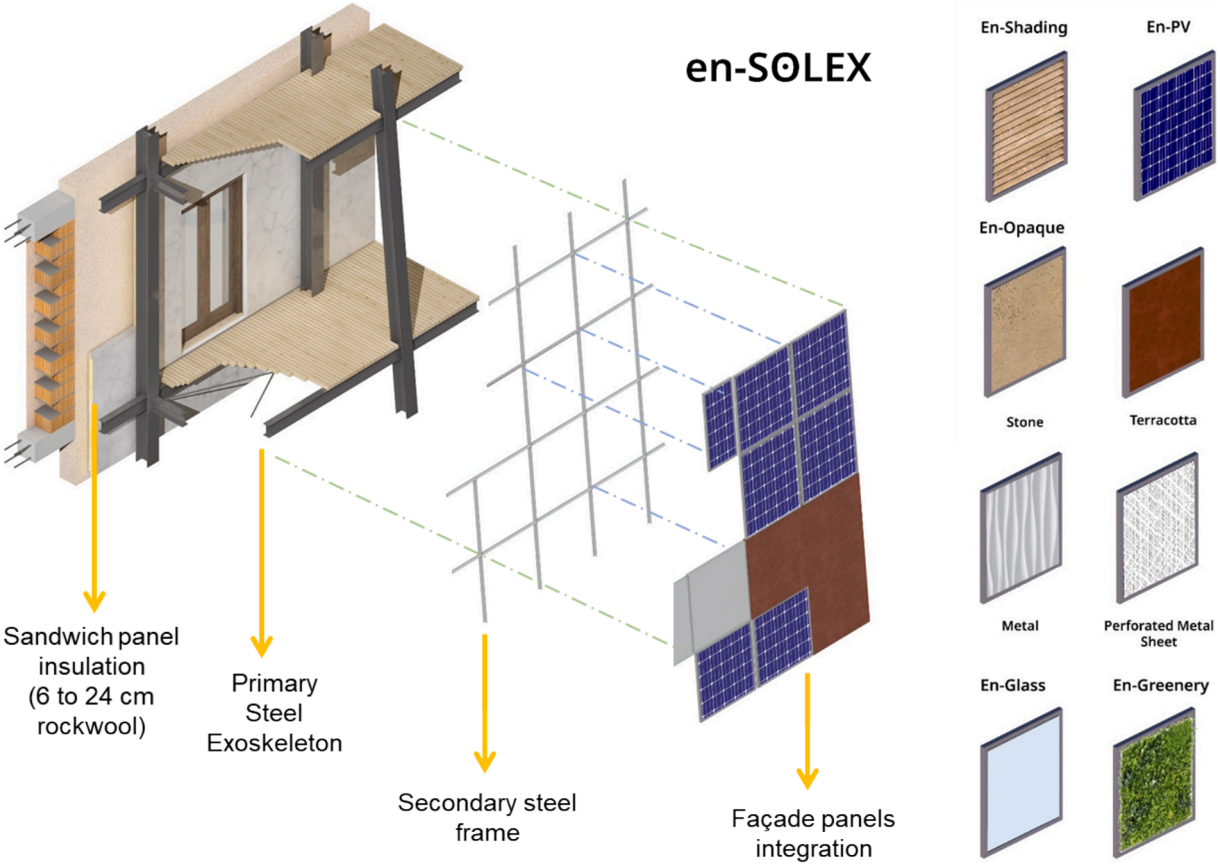

Fig. 2. The "en-SOLEX" system facade design.

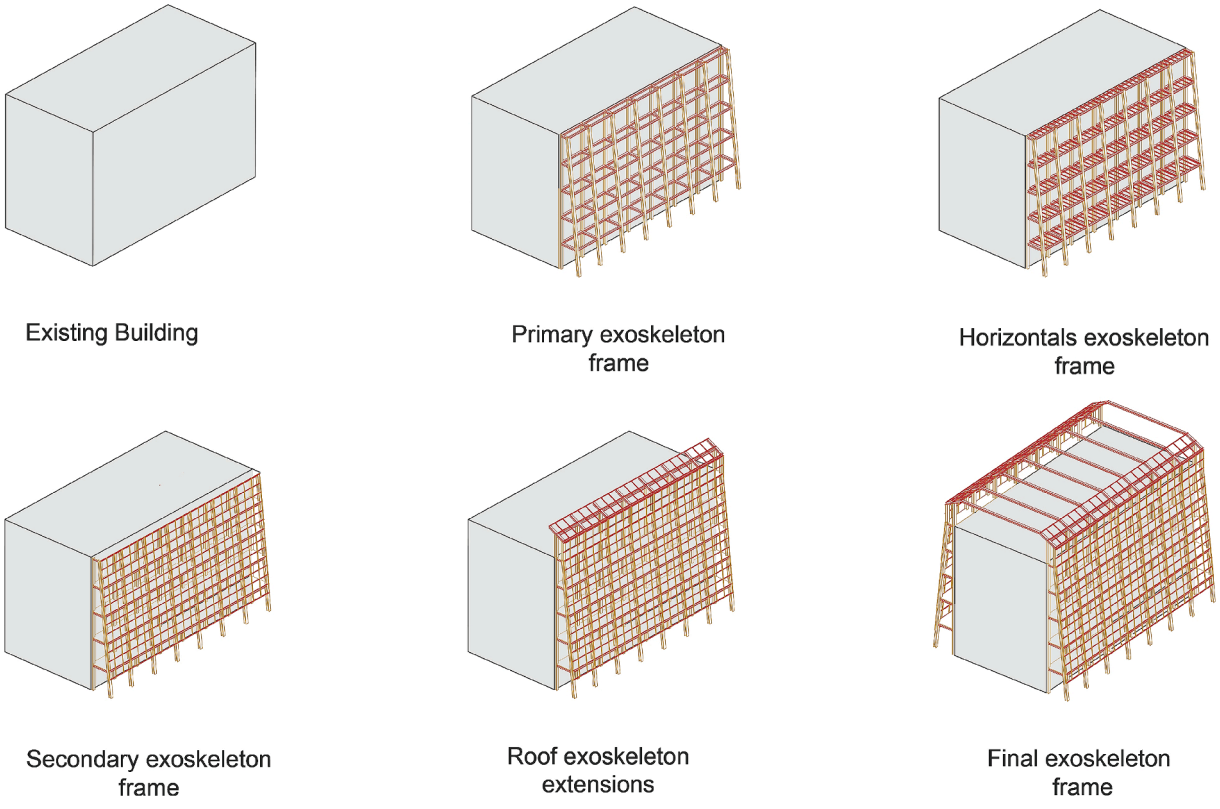

Fig. 3. The" en-SOLEX" steel frame construction steps.

building height of 21 m), while simultaneously increasing the photovoltaic panels' productivity.

In addition to the main structure, a secondary grid consisting of steel T-section profiles is employed. This secondary grid forms a 1 m x 1 m matrix, facilitating the placement of diverse panels. The module size of 1 m was taken considering the minimum height for a balcony parapet. Wooden horizontal beams are integrated into the main frame at each floor level to create supplementary external zones. These extra spaces create liveable areas such as greenhouses, balconies, or verandas that may act as buffer zones between the building's interior and exterior, further enhancing the thermal comfort experienced by occupants within the building, lowering summer temperatures, moderating winter temperatures, and improving indoor thermal comfort [38,74–77].

The modularity of the primary structural grid allows for adaptation to varying inter-storey heights of the building without alteration to the secondary grid frame, thereby reducing the design process of the system. The exoskeleton frame wraps around the building like a second skin, including the roof of the building with a truss beam frame that can hold the structural load of PV and solar thermal panels (Fig. 3).

The self-supporting frame of the system allows the panels' weight to be supported directly by the structure, avoiding any additional loads on the existing structure. This is especially crucial as the existing structure may not be able to withstand the additional loads of RES integration, particularly in terms of seismic vulnerability.

The grid's inner frame, which stands parallel to the existing building facade, is designed to integrate thermal insulation sandwich panels made of rockwool with metal cladding. The thickness of the panels can vary from 6 to 24 cm, depending on the building's energy needs and climatic zone with a ranging thermal transmittance from 0.61 to 0.09 W/m^2K.

The exoskeleton's modularity enables the use of a pre-defined technological curtain wall that can be customised through a range of possible configurations. These configurations can be modified to suit the specific intervention site and orientation. As a result, the secondary frame can be equipped with a predefined kit of prefabricated panels. Each panel has a surface area of 1 square metre and is equipped with specific anchors for easy attachment to the secondary frame, reducing the time and cost of intervention. An illustrative technical detail drawing of the module, module anchors and system frame is provided in Appendix 1 for reference.

Five different classes of modules have been designed for different functions: firstly, the En-PV module, comprising a photovoltaic panel

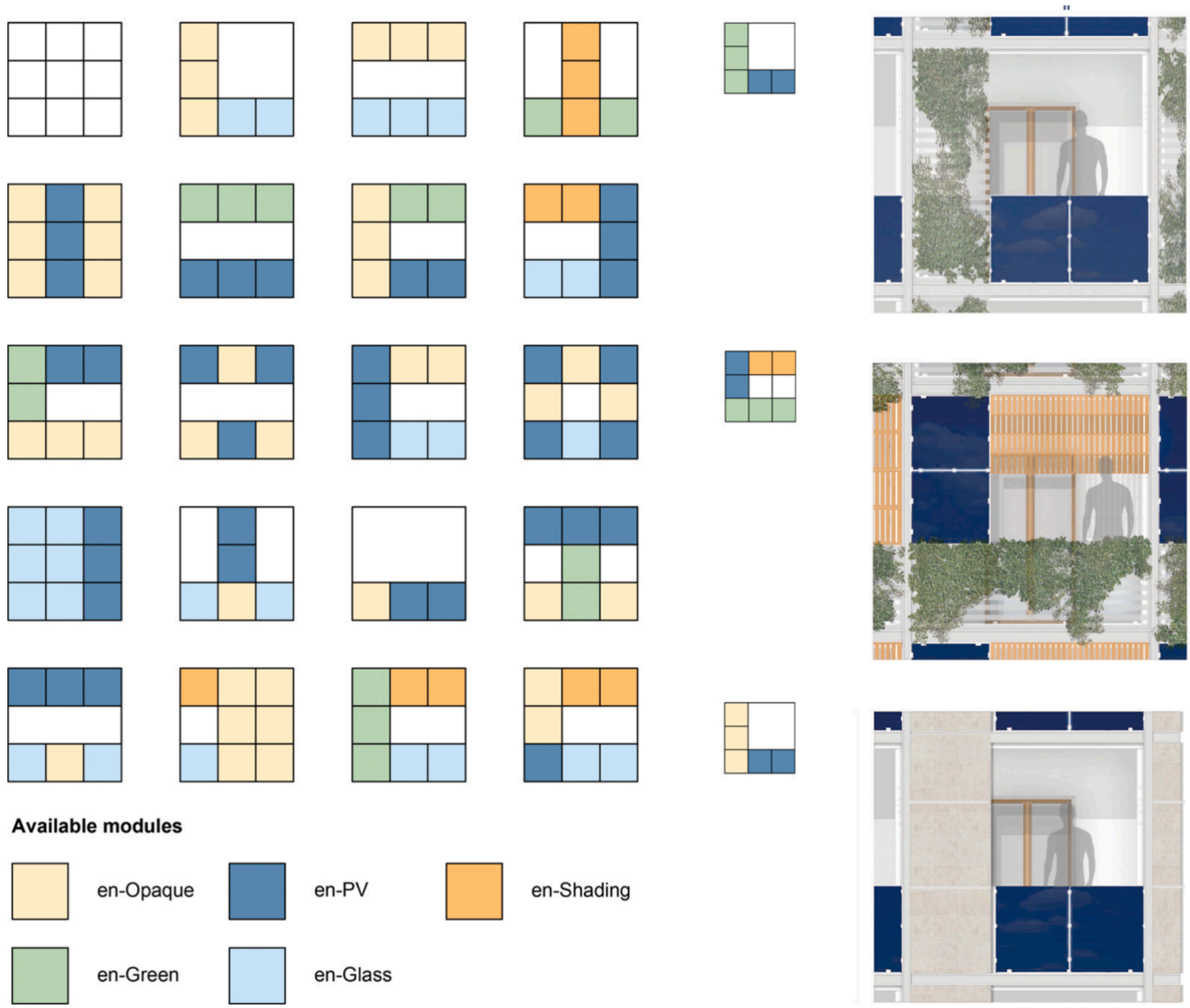

Fig. 4. Some combinations of different modules and examples of kit configurations.

with an approximate surface area of 1 m^2 and a peak power output of 200 W_p; secondly, the En-Opaque module, showcasing a variety of opaque panels crafted from porcelain stoneware, earthenware, or stone. Thirdly, the En-Glass module is made of laminated tempered glass. Fourthly, the En-Shade module offers options for horizontal or vertical brise-soleil crafted from wood or aluminium. Lastly, the En-Green module presents a pre-assembled solution tailored for low-intensity greenery integration. The combination of the façade panels thanks to its modularity and flexibility can be adapted to fit the orientation of existing buildings and the site's climatic conditions based on building energy demand (Fig. 4).

In particular, the En-PV module is selected created on its dimensions, which were already present on the market, to reduce the system cost. This module allows for the integration of RES in both the façade and the roof, thereby ensuring the necessary coverage of building energy demand.

Their positioning is mainly reserved for facades exposed to the South, to optimise the efficiency of the photovoltaic system.

The En-Opaque and En-Shading modules are developed with the specific objective of providing the required shading effect to reduce the solar radiation load during the cooling season, particularly in low-latitude locations. The En-Opaque modules provide fixed shading, while the En-Shading modules are equipped with adjustable horizontal or vertical brise-soleil according to the orientation of the building façade, to maximise the shading effect during the cooling period and minimise it during the heating season. The horizontal module should be installed on the South side, while the vertical module should be installed on the East and West sides.

Furthermore, the En-Glass module is designed to enclose the exoskeleton area in front of the windows, thereby minimising the reduction in daylight. Alternatively, it can be employed to create a bioclimatic greenhouse [78,79]. The operational mode of the greenhouse should be carefully analysed according to the orientation and the season period to avoid overheating risk. The En-Green module is proposed as a shading or wind barrier alternative to enhance the biophilia effect [80] and mitigate the urban heat island effect [81], despite the higher maintenance costs [82,83].

Both the structural grid elements and the panel types are designed to be modular and prefabricated. To ensure the adaptability of the exoskeleton structure to varying building dimensions, the panel modules have been designed with specific sub-modules measuring 0.25 x 1 m and 0.50 x 1 m. The system can be easily and quickly assembled from the outside of the existing building without affecting building occupancy and reducing the time and cost of its implementation. The modularity of the external facade grid allows for easy upgrades and adjustments to the facade modules without compromising the overall system.

The proposed retrofitting system can significantly reduce its environmental impact as each element can be easily removed, fixed, or changed to meet changing energy and design needs. Furthermore, the system can be easily dismantled and its components reused in other retrofitting interventions. Moreover, the exoskeleton structure allows for the incorporation of external lifts or fire escapes, thereby providing a potential solution to architectural barriers and safety issues in existing buildings. Fig. 5 shows the application of the "en-SOLEX" system to an existing residential building block. As can be seen, the system allows various façade designs, resulting in a unique and targeted outcome for each building.

3. Case study

To evaluate the potential energy performance achievable through the retrofit system, energy dynamics simulations were carried out on a multi-storey building belonging to a social housing residential cluster located in a southeastern suburb of Bari, Italy. The case study building is part of a residential apartment blocks built in the 1970 s, consisting of a total of seven multi-family buildings with 6 to 8 storeys. The analysis was conducted on a six-storey south-facing building with a plan length of 18 m and a depth of 11 m (Fig. 6).

Each floor contains two mirrored apartments, each measuring 78 square meters, resulting in a total of ten apartments within the building (Fig. 7).

Table 1 shows the key building and site characteristics. The building has a reinforced concrete frame structure with a 25-cm-thick reinforced concrete slab lightened with hollow bricks. The external walls are made of hollow bricks ($\lambda = 0.4$ W/mK) without insulation and plastered on both sides, with an overall thickness of 30 cm and a thermal transmittance of 1.15 W/m^2K. The flat roof consists 25-cm-thick reinforced concrete slab lightened with hollow bricks and it lacks insulation. Gypsum plaster is present on the inner side, and the roof is covered with bitumen waterproof membrane over a slope screed made of lightweight concrete. This results in an overall thermal transmittance of 1.45 W/m^2K.

Windows are made of aluminium frames without thermal breaks and incorporate double glazing filled with air, characterized by an overall thermal transmittance of 3.70 W/m^2K and a $g_{gl,n}$ of 0.75. The building has an overall net conditioned area of 818.4 m^2 and an overall net conditioned volume of 2197.5 m^3, resulting in a surface-to-volume ratio of 0.38. The plant system features an autonomous heating system for each apartment, which includes a standard boiler supplied by natural gas and installed outside. The system has an average seasonal efficiency (η_H) of 0.85 and feeds water aluminium radiators ($T_u = 80$ °C) in each room. For summer air-conditioning, several split air-conditioners with an EER of 2.7 are installed. The case study was chosen according to Section 2. It represents the target building for the implementation of the proposed retrofitting measure. It is a multi-storey apartment blocks with a rectangular shape, a linear external profile and a regular structural grid. It falls into the class 6 of the TABULA project, it was built between the 1975 and 1990 period and it is characterised by high energy

Fig. 5. Examples of possible retrofitted façade using the en-SOLEX system.

Fig. 6. Urban framework of the case study on the left and view of case study residential buildings cluster on the right.

Fig. 7. Typical floor plan of the case study on the left and south façade on the right.

Table 1
Site climatic properties and case study building features.

Climatic characteristics		
Latitude	°	N 41°7′45″
Longitude	°	E 16°52′11″
Minimum Dry Bulb Temperature	°C	0 (11th Jan.)
Maximum Dry Bulb Temperature	°C	39 (10th Aug.)
Climatic zone (D.P.R. 412/93)	–	C
Heating Degree Days	(°C·d)/yr	1185
Max direct solar radiation	W/m^2	932 (25th May)
Building Features		
Net conditioned building area	m^2	818.4
Net conditioned building volume	m^3	2197.5
Surface-to-volume ratio	m^{-1}	0.38
Scattering surface	m^2	1723.15
Windows-to-wall ratio	%	26

demand.

4. Methodology

To evaluate the energy benefits of the retrofitting measure, a dynamic simulation of the overall building-plant system analysis on an hourly basis was performed in DesignBuilder Software v. 7.2.0.6, using the *EnergyPlus* simulation engine. The existing building is firstly modelled in its current state to provide a baseline scenario.

The building energy model (BEM) is calibrated by comparing the energy consumption of the simulated building with the measured energy consumption from the natural gas and electricity bills over the last three years. The calibration of BEM is conducted according to option D of ASHRAE Guidelines 14–2023. The model is calibrated if the mean bias error (*MBE*), calculated as in Eq.1, between the measured and simulated values on a monthly basis is less than or equal to ± 5 % and the coefficient of variation (*CV(RMSE)),* defined as in Eq. (2), is less than or equal to 15 %.

$$MBE = \frac{\sum_{period}(M-S)_{month}}{\sum_{period}(M)_{month}} \times 100[\%] \quad (1)$$

$$CV(RMSE_{month}) = \frac{RMSE_{month}}{A_{month}} \times 100[\%] \quad (2)$$

Where *M* and *S* refer to measured and simulated monthly data, *RMSE* is the root mean square error on a monthly basis and *A* is the average value of measured data.

As the main aim of the system, compared to the other existing exoskeletons, is to maximise the RES integration and the on-site energy production, the simulated scenarios focused on maximising the En-PV modules implementation on the façade surface according to the

possible windows-to-wall ratio (WWR) scenarios and building energy need. Specifically, three different en-SOLEX south façade configuration scenarios were performed (Fig. 8). The first scenario, RC50, consists of a south-facing façade with a RES coverage of 50 % of the total façade area.

Considering the ASHRAE 90.1 recommendation of 24–30 % WWR, this façade configuration is suitable for buildings with up to 40 % WWR. The southern exoskeleton façade is equipped with a total of 180 En-PV modules for a total peak power of 36 kW_p, 48 En-Opaque modules and 48 En-Glass modules. En-Glass modules are used as the parapet, while the other available grid areas are fitted with En-Opaque modules to simulate the limits of building energy performance conditions based on system integration. As fixed shading, the En-Opaque modules maximise solar radiation load reduction during the cooling season, while minimising solar gain during the heating season.

The second scenario, RC30, considers a RES coverage of 30 % of the total façade area. This façade configuration uses 108 En-PV modules for a total peak power of 21.6 kWp, 120 En-Opaque modules and 48 En-Glass modules and can be applied to buildings with a WWR of up to 60 %. The final scenario, RC20, is characterised by a 20 % RES coverage with a total of 72 En-PV panels, 156 En-Opaque modules and 48 En-Glass modules. This façade configuration is suitable for buildings with up to 80 % WWR.

All scenarios consider the application of 8-cm-thick sandwich panels directly to the external wall on both sides of the exoskeleton, to achieve the thermal transmittance threshold foreseen by Italian regulation for climatic zone C [84]. The east and west sides of the building were considered adiabatic, as the building exhibits two blind sides in common with the other residential block buildings, thus no additional insulation was provided.

All the scenarios are equipped with the same northern exoskeleton façade made by the same combination of En-Opaque, En-Glass and En-Green modules. Although the northern façade of the exoskeleton does not contribute directly to improving the energy performance of the building, and its use may not be cost-effective in terms of a cost-benefit analysis, since it has to symmetrically support the load of the metal roof exoskeleton structure, it was decided to equip it with a series of panels that can make the retrofit harmonious. Also, the roof configuration is kept constant among the scenarios. A total of 100 En-PV modules are installed on the roof frame providing a total of 20 kW_p. Additionally, the upper part of the exoskeleton tilted at 30°, allows for the integration of 34 m^2 of solar thermal panels.

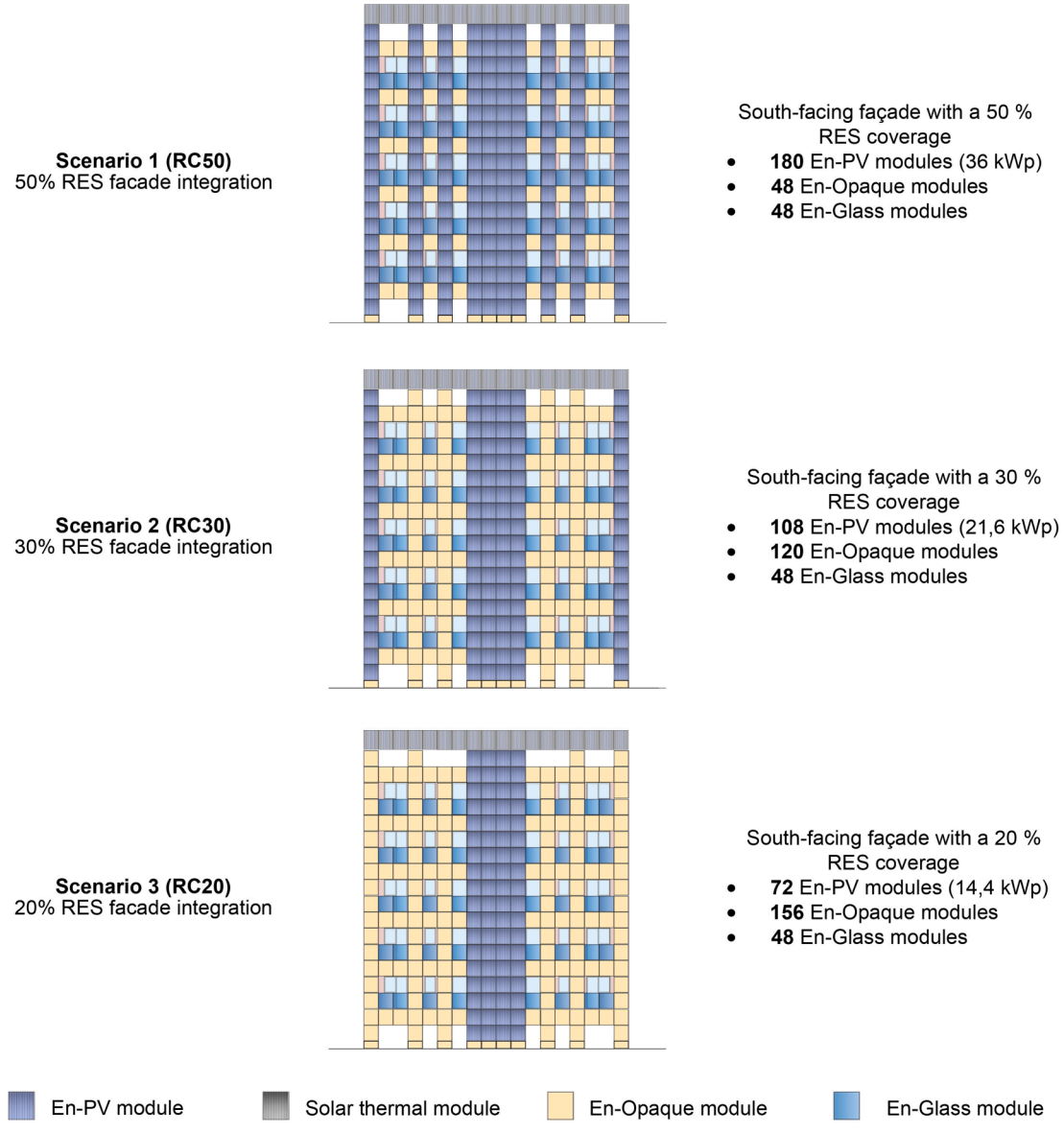

Fig. 8. Representation of the different scenarios analysed based on the configuration of the south façade of the en-SOLEX system.

4.1. Simulation input

The IGDG weather data for Bari-Palese were used. The setpoint temperature was fixed at 20 °C for the heating period and 26 °C for the cooling period according to requirements for residential buildings consistent with category II of UNI EN 16798–1. The heating and cooling system schedule was set to be always available (24 h per day). The energy needs for heating, cooling, ventilation, hot water production, lighting, and appliance electrical needs and the PV energy generation were assessed.

Based on the available beds in the apartments, an occupancy of 4 people for each apartment is considered, for an overall occupancy of 40 people. Scheduled daily occupancy and internal heat gain for the different thermal zones used in the simulation are summarized in Table 2.

The lighting system has a power density of 2.5 W/m^2-100 lx. The infiltration rate of the model is set at 0.5 h^{-1}. Natural ventilation ranges from 5 to 12 vol/h and is activated when the indoor temperature ranges from 21 °C to 25 °C. To prevent overheating or overcooling, a temperature differential of 1 °C between indoor and outdoor temperatures has been set in the simulations.

Seven simulations were performed. The first simulation analysed the building energy consumption without integrating the en-SOLEX system, serving as a baseline scenario. Only shading provided by the existing balconies was considered.

The next three simulations evaluated the en-SOLEX integration based on three different façade configuration scenarios (Fig. 8). The final three simulations involved the first three scenarios RC50, RC30 and RC20 combined with the replacement of the existing gas boiler with a centralised air-to-water heat pump (COP = 4.0 and EER = 5.2) with fan coil units to achieve complete electrification of the building's energy needs (Fig. 9). To assess the variability of heat pump behaviour as a function of the temperatures the *ASAP HighT COPFT curve* for heating mode and *AirCooled CentEIRFT* available in the EnergyPlus database were implemented.

To describe the matching degree between on-site energy generation and the building load, the load match index f_{load},[85] is defined as the average value over an evaluation period of how the on-site generation covers the energy load was evaluated following Equation (3).

$$f_{load} = 1/N \cdot \Sigma_{year}(min[1, g(t)/l(t)]) \quad (3)$$

where $l(t)$ represents the energy load, $g(t)$ *is* the onsite electricity production, and N is the number of samples in the evaluation period. If hourly resolution data is used for a complete year evaluation period, there will be 8760 samples.

Finally, to evaluate the positive target of the building thanks to the retrofitted system integration, the difference between the energy exported from the building to the grid, $e(t)$, and the energy supplied, $d(t)$, known as the net exported energy, represented by $ne(t)$, is evaluated according to Equation (4) [85]:

$$ne(t) = e(t) - d(t) \quad (4)$$

Table 2
Scheduled daily occupancy and internal heat gain for each thermal zone.

Thermal zone	Occupancy daily time		Appliances and occupancy load [W/m^2]	
	From Monday to Friday	Weekend	From Monday to Friday	Weekend
Master bedroom	from 10 p.m. to 8 a.m.	from 10 p.m. to 10 a.m.	2.67	3.58
Double bedroom	from 6 p.m. to 8 a.m.	from 10 p.m. to 9 a.m.	2.67	3.58
Living room	from 8 a.m. to 10 a.m. from 4 p.m. to 12 a.m.	from 9 a.m. to 11 a.m. from 4 p.m. to 12 a.m.	9	9
Kitchen-Dining room	from 7 a.m. to 9 a.m., from 12 p.m. to 2 p.m. from 8 p.m. to 10 p.m.	from 7 a.m. to 9 a.m., from 12 p.m. to 2 p.m. from 8 p.m. to 10 p.m.	9	9

5. Results

5.1. Energy analysis of the baseline scenario

According to the dynamic simulation results, the building has a total energy consumption of 76,953.1 kWh/year. Natural gas powers 66 % (50,730.3 kWh/year), while the remaining 34 % (26,223.2 kWh/year) is supplied by grid electricity (Fig. 10).

The building heating (H) and domestic hot water (DHW) are supplied by natural gas, accounting for 59 % (45,435 kWh/year) and 7 % (5,295.3 kWh/year) of the total energy consumption, respectively. The other building services are supplied by grid electricity. Cooling (C) accounts for 6 % (4.177,3 kWh/year), interior lighting for 7 % (5,658.7 kWh/year) and interior equipment for 21 % (16,386.9 kWh/year).

When comparing the simulated energy consumption with the energy bills as described in section 4 (Fig. 11), it was found that the average electricity consumption was lower than the simulated value, resulting in 25,570 kWh/year. However, the natural gas consumption was higher than the simulated one, resulting in an overall natural gas need of 52,379 kWh/year. Specifically, the monitored electricity consumption is observed to be lower than the simulated throughout the year, except during the cooling months, where higher intensity use of cooling systems is evident. Conversely, the consumption of natural gas was observed to exceed the simulated value during the heating season, whereas it subsequently declined as the heating period ends.

The resulting MBE accounts −1.4 % for electricity and 3.1 % for natural gas. The CV(RMSE$_{month}$) was 13.3 % for electricity and 14.6 % for natural gas. Both indices are consistent with the ASHRAE 14–2023 limits. Therefore, the simulation model can be considered calibrated.

Table 3 provides the total yearly energy consumption and per square meter for each building service.

5.2. Comparison of en-SOLEX system scenarios

Fig. 12 shows the monthly comparison of heating and cooling consumption between the base case and retrofitted scenarios. The integration of the en-SOLEX system results in a significant reduction in heating and cooling needs in all analysed scenarios. Compared to the baseline scenario, scenarios RC50, RC30 and RC20 all show a reduction in energy consumption for both cooling and heating. The heating and cooling energy savings are almost the same for the three scenarios, as the passive measures characteristic doesn't change depending on the scenario.

The heating energy consumption in the three scenarios is reduced by 33 % compared to the base case while cooling needs are reduced by up to 25.9 % (Table 4). The heating energy requirement is primarily reduced by integrating additional insulation into the external wall. Conversely, the reduction in building cooling energy needs is mainly due to the exoskeleton shading systems reducing summer solar loads.

The benefit of the retrofit measure is more evident when combined generator replacement as in the RC50 + HP, RC30 + HP and RC20 + HP scenarios, resulting in maximum heating and cooling reductions of up to 80.7 % in the RC50 + HP scenario and up to 60.5 % in the RC20 + HP scenario.

As can be seen in Fig. 13, the incident solar radiation is greatly reduced by the shading effect of the retrofit measure, especially during the summer period, from a maximum of 0.68 kW/m^2 to 0.21 kW/m^2 reducing the cooling energy needs of the building.

The loss of solar gain due to the shading effect of the system, during the winter period, is compensated by the reduction in the transmittance

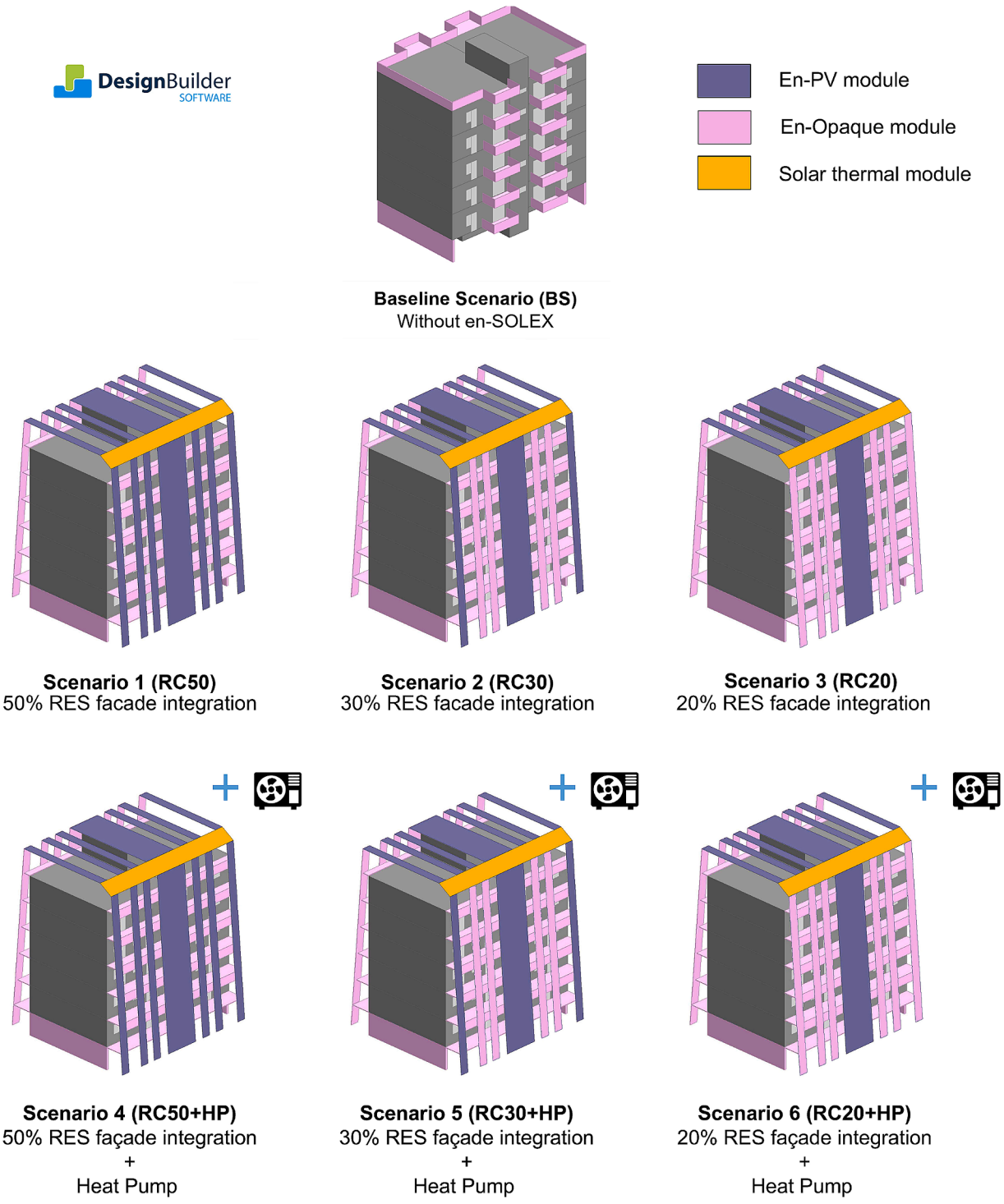

Fig. 9. Design builder 3D model for each analysed scenario.

of the vertical walls achieved by the introduction of insulation in the façade. In any case, the lower inclination of the sun rays during the winter period does not significantly reduce the radiation on the window components, whose values are slightly lower than those of the baseline scenario. As a result, even the indoor operative temperatures and especially the mean radiant temperature of the building, during the summer period, are significantly reduced.

Fig. 14 shows the comparison of the hourly variation of operative temperatures and mean radiant temperatures for a typical summer week (20–27 July) in a free-running simulation between the base case and the RC50 scenario for a master bedroom on the 3rd floor facing southwest. Compared to the base case scenario, the en-SOLEX system produces a reduction of up to 2.03 °C in the operating temperature (on 21 July at 10.00) and 2.14 °C in the mean radiant temperature (on 21 July at 9.00) improving the thermal comfort within the building and increasing the thermal building resiliency. This effect can also be investigated by conducting a comprehensive indoor thermal comfort evaluation throughout the year, by the acceptability limits set in Category II of the EN 16798–1 standard [86]. As evidenced in Table 5, the en-SOLEX system is effective in reducing the overall number of unmet hours. In

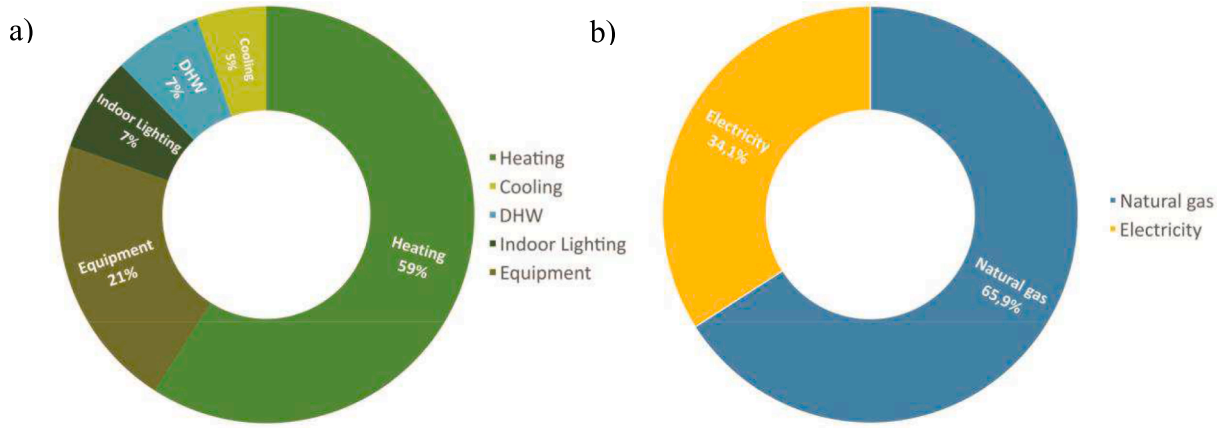

Fig. 10. Baseline building energy consumption by energy service (a) and by energy vector (b).

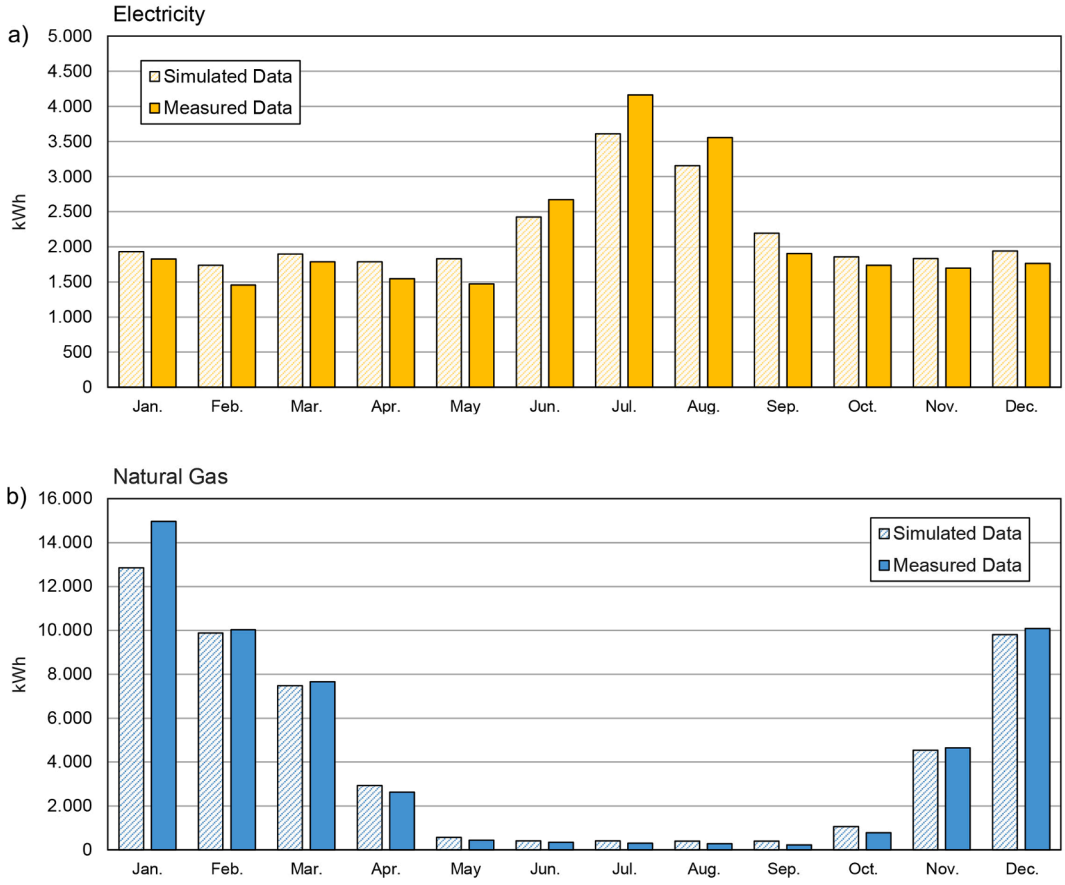

Fig. 11. Energy consumption comparison between simulated and measured data on a monthly basis for electricity (a) and natural gas (b).

Table 3
Yearly energy consumption for each building service.

Services	Total energy consumption		Total energy consumption per square meter		%
Heating	45,434.9	kWh/year	55.53	kWh/m^2 year	59 %
Cooling	4,177.3	kWh/year	5.11	kWh/m^2 year	6 %
DHW	5,295.3	kWh/year	6.47	kWh/m^2 year	7 %
Indoor Lighting	5,658.7	kWh/year	6.92	kWh/m^2 year	7 %
Equipment	16,386.9	kWh/year	20.03	kWh/m^2 year	21 %
Total energy	76,953.1	kWh/year	94.05	kWh/m^2 year	100 %

particular, with regard to the various thermal zones in the southwest-facing apartment on the third floor, a reduction in discomfort hours ranging from 23 to 38 % was observed when comparing the baseline scenario to the retrofitted one. The greatest reduction was observed in the master bedroom, followed by the living room, where the reduction was 33 %. The kitchen exhibited a percentage reduction of 31 %, while the double bedroom demonstrated an overall reduction of 23 %.

5.2.1. *Electricity generation of en-SOLEX system scenarios*

In terms of PV energy production, scenario RC50 generates a total of 55,426.5 kWh/year, while scenario RC30 generates 43,063.4 kWh/year and scenario RC20 generates 36,863.3 kWh/year. The electricity

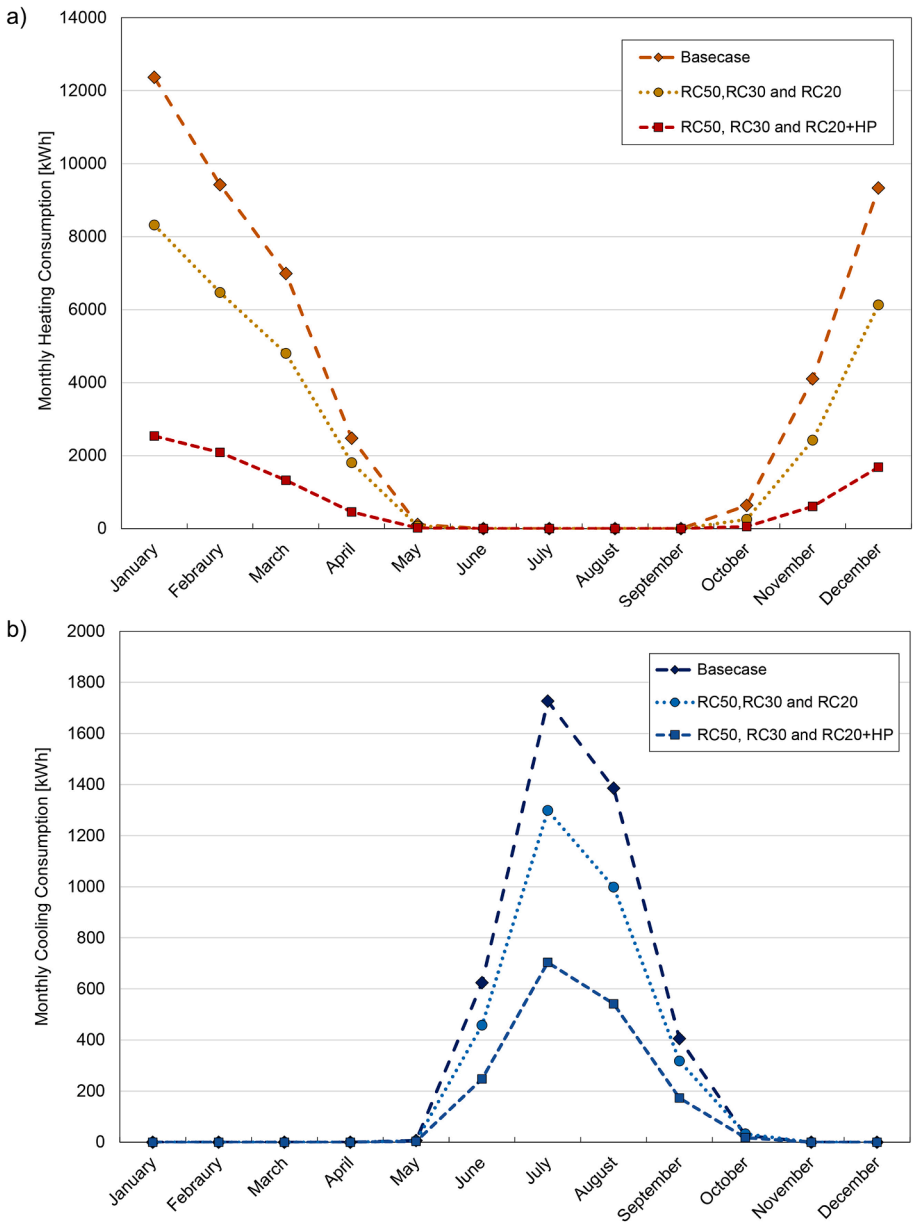

Fig. 12. Monthly heating (a) and cooling (b) energy consumption among analysed scenarios.

Table 4
Heating and cooling energy consumption comparison among scenarios.

Scenario	Heating energy consumption		Cooling energy consumption	
	kWh/year	Δ%	kWh/year	Δ%
Base case	45,435.0		4,177.2	
RC50	30,277.6	*–33.4 %*	3,111.5	*–25.5 %*
RC30	30,399.9	*–33.1 %*	3,098.0	*–25.8 %*
RC20	30,433.6	*–33.0 %*	3,094.7	*–25.9 %*
RC50 + HP	8,774.0	*–80.7 %*	1,687.9	*–59.6 %*
RC30 + HP	8,813.2	*–80.6 %*	1,668.6	*–60.1 %*
RC20 + HP	8,896.1	*–80.4 %*	1,651.7	*–60.5 %*

supplied by PV placed on the roof remains constant in all simulations and accounts for 43.7 %, 56.2 %, and 65.7 % of total generation for scenarios RC50, RC30, and RC20, respectively (Table 6). In all RC scenarios, on-site generation exceeds the building energy needs compared to the base case electricity requirements. Scenario RC50 covers the building electricity consumption by 225.4 %, RC30 by 175 %.1 and RC20 by 150 % (Table 8).

When considering the building's total energy consumption with the share of natural gas, the RES coverage decreases, reaching values of 101.1 % in the RC50 scenario, 78.5 % in the RC30 scenario and 67.2 % in the RC20 scenario.

Based on the reference case electricity consumption (Fig. 15), scenario RC50 covers the monthly building electricity needs for the entire year. Scenario RC30 covers the monthly electricity consumption from February to November, while scenario RC20 covers the monthly electricity consumption from April to October.

Focusing on the en-SOLEX system combined with heat generator replacement scenarios, which provides full electrification of the building's energy needs, as the RES percentage on the façade decreases, the energy consumption covered by the renewable source drops.

The RC50 + HP scenario covers the total energy consumption from March to November, the RC30 + HP scenario from March to October, and the RC20 + HP scenario only from April to October. However, despite the increased building electricity need, scenario RC50 + HP still generates 165.2 % more electricity than the building requires, while

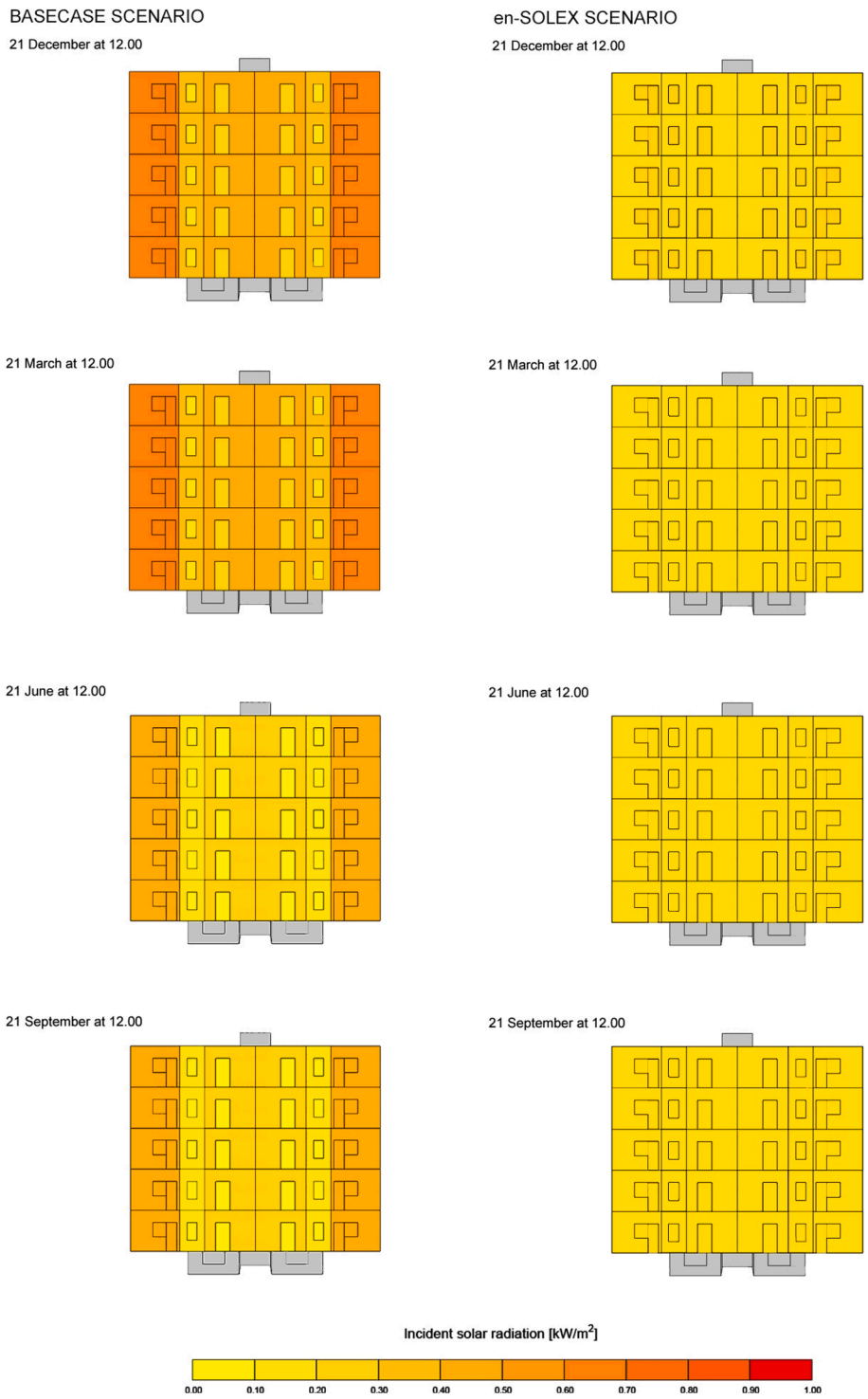

Fig. 13. Incident solar radiation on the South facade at noon comparison between base case scenario and en-SOLEX one on 21 December, 21 March, 21 June and 21 September.

scenario RC30 + HP generates 135 %. On the other hand, scenario RC20 + HP covers 69.5 % of the building's energy consumption.

Although the total energy produced on site is significantly higher than the building's energy needs in almost all scenarios, there is a mismatch between hourly production and consumption throughout the year, particularly in winter. The annual load match index on an hourly basis ranges from 41.7 % in scenario RC20 + HP to 44.7 % in scenario RC50 (Table 7).

Table 8 shows the comparison between building energy consumption, building electricity generation, *g(t),* the amount of exported *e(t)*, delivered electricity *d(t)* and self-consumed electricity *s (t)*. The data shows that scenario RC50 exported 170 % of generated electricity, RC30 exported 126.7 % and RC20 exported 105.1 %. On the other side, scenario RC50 + HP exported 129.6 %, scenario RC30 + HP 95.8 % and scenario RC20 + HP 79.4 %. Based on the building's energy needs, higher electricity production leads to a higher level of self-consumption.

The scenario with the highest quota of self-consumption is RC50 with

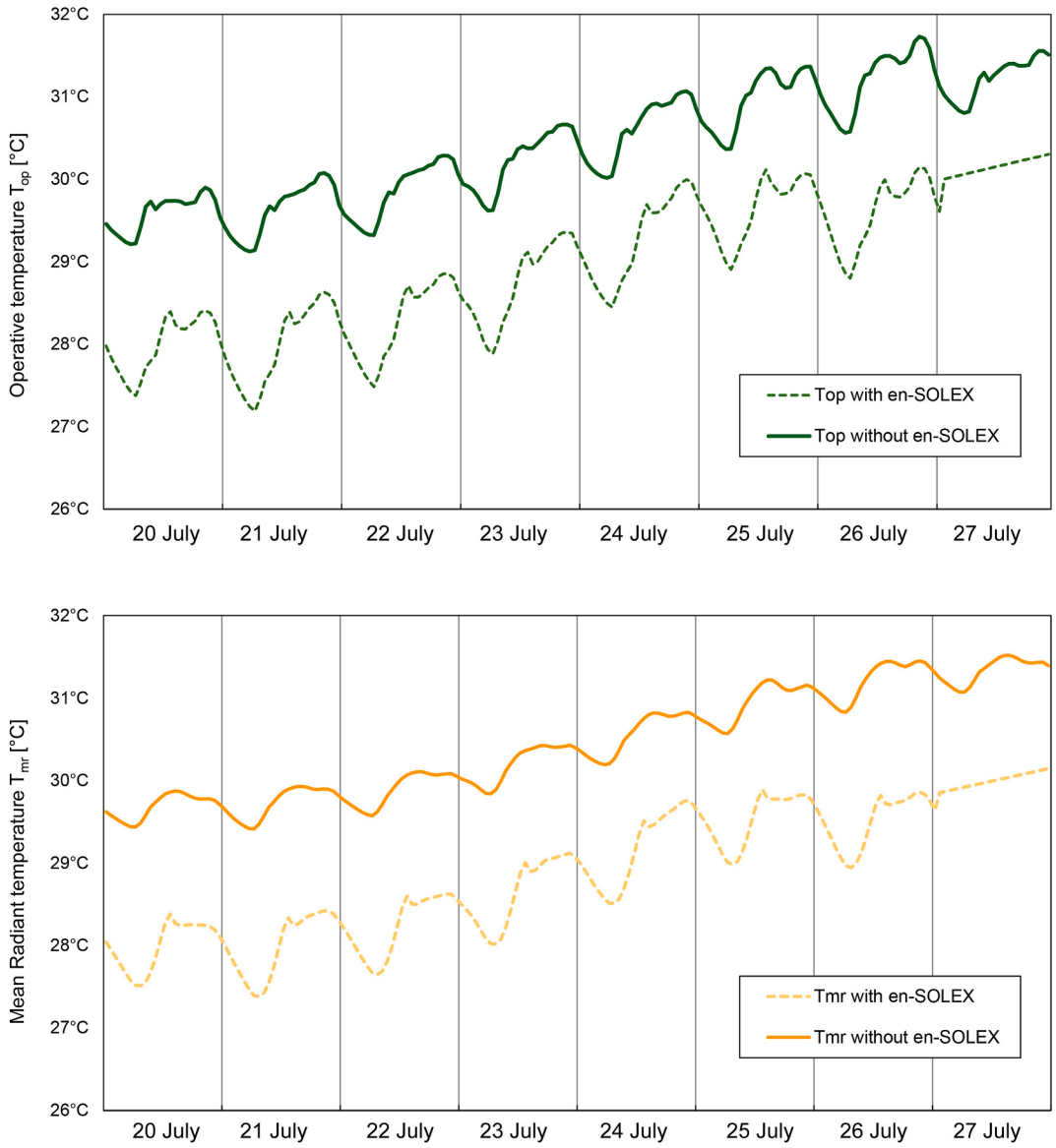

Fig. 14. Operative temperature and Mean radiant temperature variation for a typical summer week in free-running mode between the base case and "en-SOLEX" retrofitted solution.

Table 5
Unmet hours according to EN 16798–1 Category II acceptability limit.

		Without en-SOLEX	With en-SOLEX	Δ%
South-West	Master Bedroom	1596.5	995.0	−38 %
	Kitchen	960.0	659.5	−31 %
	Double Bedroom	1596.5	1222.0	–23 %
	Living Room	968.0	646.5	–33 %

Table 6
PV electricity production by roof and façade for each scenario.

Scenario	PV electricity production	
	Roof	**Facade**
RC50	43.7 %	56.3 %
RC30	56.2 %	43.8 %
RC20	65.7 %	34.3 %

43.2 %, followed by the RC50 + HP scenario with a share of 35.5 % for the heat generator replacement scenarios. When comparing scenarios with the same RES coverage, those with only the en-SOLEX system exported more electricity to the grid. The amount of electricity exported ranged from 42,033.7 kWh in scenario RC50 to 25,831.1 kWh in scenario RC20.

Based on the en-SOLEX façade configuration, as the total on-site electricity generation decreases, the amount of electricity from the grid increases, reaching up to 67.5 % with scenarios RC30 + HP.

Looking at the net electricity balance (*ne(t)*) between the building and the grid, it can be seen that all the retrofit scenarios result in a positive balance between the electricity exported and the electricity supplied by the grid. Specifically, the RC50 scenario results in a net balance of 114.1 %, the RC30 scenario 66 % and the RC20 scenario 42.5 %. Even with the full electrification of building energy needs the net balance remains positive ranging from 65.2 % with scenario RC50 + HP to 9.9 % with scenario RC20 + HP, turning the retrofitted building into a positive one.

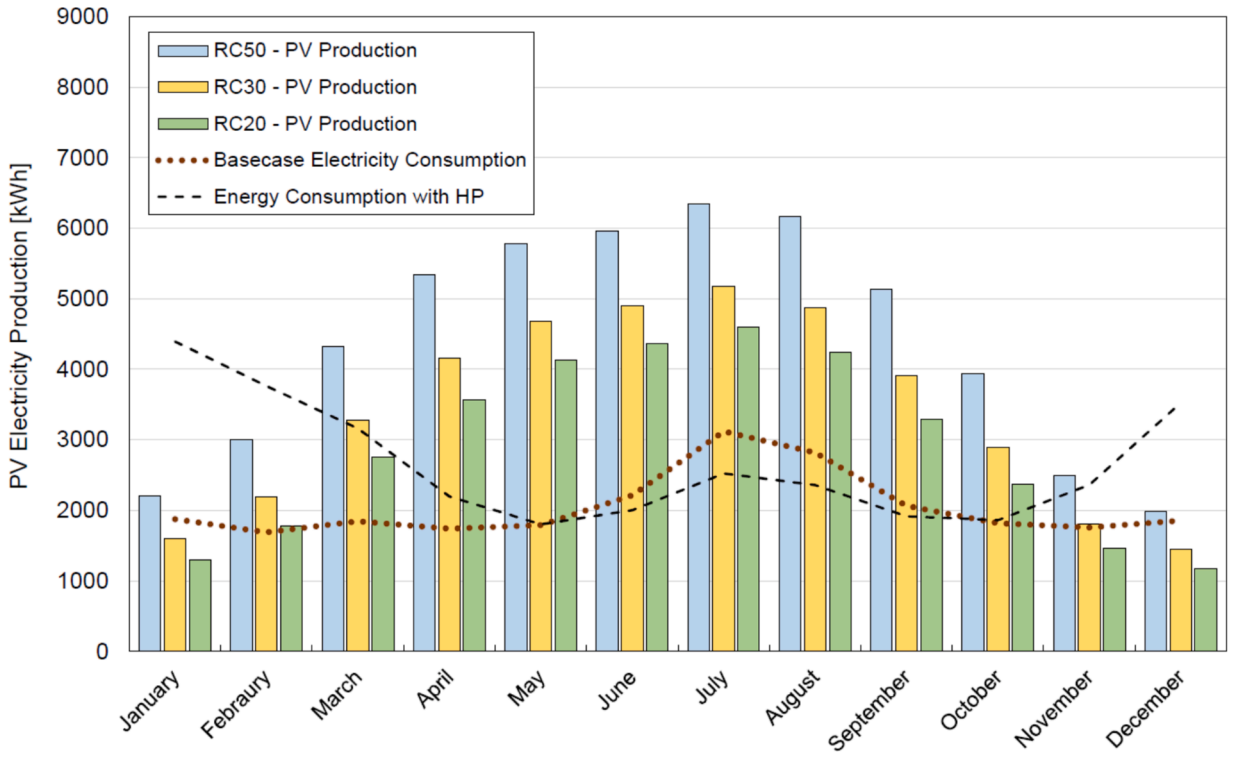

Fig. 15. Comparison of the monthly electricity consumption between the base case scenario and the retrofitted scenario PV production.

Table 7
Yearly, Monthly and Hourly Load match index among scenarios.

	Scenario	Yearly	Monthly	Hourly
Load Match Index	RC50	100 %	100 %	44.7 %
	RC30	100 %	97 %	43.1 %
	RC20	100 %	93 %	41.8 %
	RC50 + HP	100 %	91 %	43.5 %
	RC30 + HP	100 %	91 %	42.3 %
	RC20 + HP	100 %	90 %	41.7 %

5.3. Analysis of different building orientations

The optimal orientation allows for the greatest exposure to the sun, thereby enhancing energy production. However, many buildings are not positioned in ideal orientations, which can have a detrimental effect on the effectiveness of photovoltaic systems. By analysing a range of orientations, this analysis aimed to provide a more comprehensive understanding of the system's adaptability and performance in real-world conditions, where optimal solar alignment is not always possible. The same scenarios were analysed by altering the orientation of the en-SOLEX façade configuration, varying its position from east to west.

Table 9 presents a summary of the results from the analysis detailed in Appendix 2, with a focus on the electricity generated in comparison to the energy consumption of the corresponding scenarios, as well as the net electricity exported.

As can be seen, despite the non-optimal orientation, the en-SOLEX system it's able to ensure a surplus of building energy consumption and the net positive energy target. As expected, the efficiency of the photovoltaic system declines under the variation in the azimuth angle. The system reaches a limit value for PV electricity generation in the West and East sides, respectively, of 182.7 % and 180 % of the corresponding

Table 8
Generated, exported, self-consumed and delivered electricity comparison among the analysed scenarios.

Scenario		RC50		RC30		RC20	
		kWh/year		kWh/year		kWh/year	
Electricity Consumption	*l(t)*	24594.8		24584.6		24581.9	
Generated Electricity	*g(t)*	55426.5	225.4 %	43063.4	175.1 %	36863.3	150.0 %
Exported Electricity	*e(t)*	42033.7	170.0 %	31114.2	126.7 %	25831.1	105.1 %
Delivered Electricity	*d(t)*	13973.3	56.8 %	14818.6	60.3 %	15392.9	62.6 %
Self-consumed electricity	*s(t)*	10621.5	43.2 %	9766.0	39.7 %	9189.0	37.4 %
Net exported Electricity	*ne(t)*	28060.4	114.1 %	16325.7	66.0 %	10438.1	42.5 %

Scenario		RC50 + HP		RC30 + HP		RC20 + HP	
		kWh/year		kWh/year		kWh/year	
Electricity Consumption	*l(t)*	31882.5		31882.5		31882.5	
Generated Electricity	*g(t)*	55426.5	165.2 %	43063.4	135.0 %	36866.4	69.5 %
Exported Electricity	*e(t)*	41321.0	129.6 %	30555.8	95.8 %	25306.3	79.4 %
Delivered Electricity	*d(t)*	20548.3	64.5 %	21523.0	67.5 %	22165.8	62.6 %
Self-consumed electricity	*s(t)*	11334.2	35.5 %	10359.5	32.5 %	9716.7	30.5 %
Net exported Electricity	*ne(t)*	20772.7	65.2 %	9032.1	28.3 %	3140.6	9.9 %

Table 9
Generated and net exported electricity comparison among the analysed scenarios based on orientation.

Generated Electricity						
	RC50	**RC30**	**RC20**	**RC50 + HP**	**RC30 + HP**	**RC20 + HP**
East	182.0 %	147.0 %	129.2 %	143.9 %	116.0 %	102.0 %
South-East	213.9 %	167.6 %	144.4 %	165.8 %	129.9 %	111.8 %
South	225.4 %	175.2 %	150.0 %	173.8 %	135.1 %	115.6 %
South-West	213.8 %	167.6 %	144.4 %	165.8 %	129.9 %	111.9 %
West	182.7 %	147.3 %	129.6 %	144.0 %	116.1 %	102.1 %
Net exported electricity						
	RC50	**RC30**	**RC20**	**RC50 + HP**	**RC30 + HP**	**RC20 + HP**
East	72.9 %	39.6 %	22.8 %	36.7 %	10.2 %	3.1 %
South-East	103.2 %	59.3 %	37.2 %	57.5 %	23.4 %	6.3 %
South	114.1 %	66.4 %	42.5 %	65.2 %	28.3 %	9.9 %
South-West	103.1 %	59.3 %	37.2 %	57.6 %	23.4 %	6.3 %
West	73.5 %	40.0 %	23.1 %	36.8 %	10.3 %	3.0 %

scenario energy consumption. The results reveal a slight difference between the West and East orientations, with the East side showing the least effective performance. Compared to the South orientation, the East orientation experiences the highest reduction in generated electricity, ranging from 11.8 % in the RC20 + HP scenario to 19.2 % in the RC50 scenario. Notwithstanding a decrease in on-site generation, all scenarios demonstrate a net energy balance between the energy required from the grid and the energy exported of a value greater than zero, thereby achieving the objective of a positive net energy building. The lowest value, corresponding to 3 %, is observed in the east-facing RC20 + HP scenario. This outcome is due to the combination of the lowest installed capacity of photovoltaics in this scenario, along with the higher energy consumption compared to scenarios that do not include a heat pump.

Table 10 shows the PV electricity production by roof and façade for each scenario based on different en-SOLEX orientations. The analysis indicates that, despite the southern orientation typically being more favourable for photovoltaic performance, the contribution of photovoltaics integrated into the façade in other orientations remains significant.

The observed reductions in energy generation are relatively minor, indicating that façade-integrated photovoltaics can still provide an effective solution. This demonstrates the feasibility of such systems in suboptimal orientations, where the reduction in efficiency is not significant enough to negate their overall contribution to energy production.

Fig. 16 provides an overview of the percentage of generated electricity in comparison to the corresponding scenario energy consumption and of the net exported electricity according to the different en-SOLEX system orientations. In the case of the N-W, N and N-E orientations, the primary en-SOLEX façade with En-PV modules is oriented in a manner that allows it to face the sun to S-E, S and S-W, respectively.

Table 10
PV electricity production by roof and façade for each scenario based on different en-SOLEX orientations.

	RC50		**RC30**		**RC20**	
	Roof	Façade	Roof	Façade	Roof	Façade
East	48 %	52 %	60 %	40 %	68 %	32 %
South-East	43 %	57 %	55 %	40 %	64 %	32 %
South	44 %	56 %	56 %	45 %	66 %	36 %
South-West	43 %	57 %	55 %	44 %	64 %	34 %
West	48 %	52 %	60 %	45 %	68 %	36 %

5.4. Energy performance analysis of the en-SOLEX system combined with a deep renovation strategies

A final set of simulations was conducted to evaluate the combined impact of implementing the en-SOLEX system alongside deep renovation strategies on the building's energy performance. Specifically, as the replacement of the heat generator and the insulation of the external walls had already been considered, the analysis was extended to encompass a more comprehensive retrofitting approach. This included the replacement of existing windows and the insulation of the flat roof. These additional energy retrofitting measures were selected based on literature, which identifies them as cost-effective strategies for improving energy efficiency in building refurbishment actions [3,28,87]. A 78 % reduction in the flat roof's thermal transmittance, bringing it to a value compliant with the Italian standard of 0.32 W/m2K, was analysed. This improvement was achieved by considering the addition of 12-cm-thick EPS insulation panels on the flat roof stratigraphy. Additionally, the existing aluminium window frames without thermal breaks, equipped with double glazing filled with air and having an overall thermal transmittance of 3.70 W/m2K, were replaced with PVC frames incorporating thermal breaks. The new windows feature low-emissivity (LoE) double glazing filled with argon, resulting in a reduced overall thermal transmittance of 2.0 W/m2K. No additional insulation was foreseen for the East and the West sides of the building, as they are considered adiabatic in the simulation.

Table 11 provides a comparison of the heating and cooling energy savings resulting from the implementation of deep renovation strategies (indicated with "*") relative to the base case scenario and to corresponding scenarios in which these strategies are not employed.

As expected, the proposed deep renovation strategies increase the energy saving both for cooling and heating energy consumption. A percentage drop up to 83.9 % in heating and 60.3 % in cooling energy consumption is achieved by the RC + HP* scenarios compared with the base case scenario. Conversely, a lower energy saving is achieved by the scenarios without the heat generator replacement. A maximum energy saving of up to 44.9 % for heating occurs with the RC50* scenario, while scenarios RC20* and RC30* achieved the highest cooling energy saving of 27.1 %.

Consistent with the outcomes of the previous simulations, variations in façade configurations across the RC50, RC30, and RC20 scenarios primarily affect the number of installed photovoltaic modules, while the levels of shading and insulation remain constant. Consequently, the differences in performance outcomes between these scenarios are minimal, with only slight deviations observed in the results. In comparison to the corresponding scenario, the application of deep renovation strategies, primarily aimed at reducing energy losses through the building envelope, has been shown to significantly improve energy savings, particularly for heating. The most notable impact is a reduction in heating energy demand, reaching up to 17.9 %. However, these renovation measures prove largely ineffective in reducing cooling energy demand, with a maximum decrease of only 1.7 %.

The reduction in consumption leads to an increase in the energy generated and exported by the different scenarios (Table 12). In particular, the RC50* scenario achieves a maximum energy generation equivalent to 226.3 % of the building's energy consumption, while the RC50 + HP* scenario reaches up to 182.7 %. Additionally, net electricity export increases significantly, with the RC50* scenario achieving a value of 114.9 %, compared to 73.6 % in the RC50 + HP + scenario, which incorporates full electrification of the building's energy services. These results demonstrate the substantial potential of the RC50* scenario for energy self-sufficiency and surplus electricity export, while the

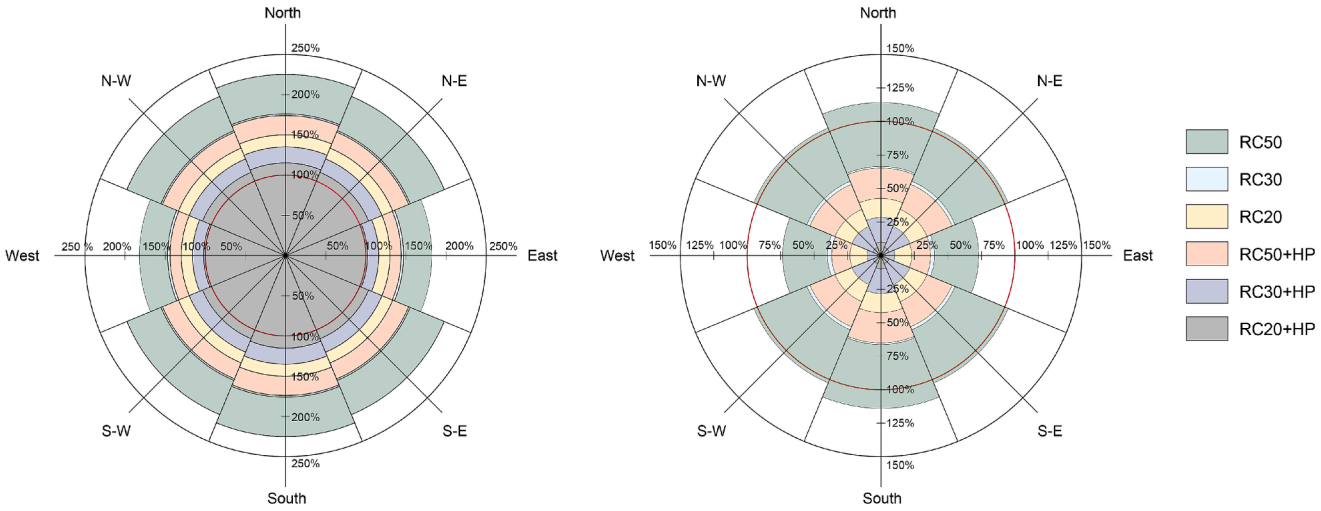

Fig. 16. Generated electricity (a) and net exported electricity (b) for each retrofitted scenario according to the different building orientations.

Table 11
Heating and cooling energy consumption comparison among scenarios with and without deep renovations strategies compared to the base case scenario.

	Heating consumption			**Cooling consumption**		
	kWh/year	Δ% compared to base case scenario	Δ% compared to the corresponding scenario	kWh/year	Δ% compared to base case scenario	Δ% compared to the corresponding scenario
Base case	45435.0	–	–	4177.2	–	–
RC50	30277.6	–33.4 %	–	3111.5	−25.5 %	–
RC50*	25026.6	−44.9 %	17.3 %	3059.5	−26.8 %	1.7 %
RC30	30399.9	–33.1 %	–	3098.0	−25.8 %	–
RC30*	25121.7	−44.7 %	17.4 %	3046.9	−27.1 %	1.6 %
RC20	30433.6	–33.0 %	–	3094.7	−25.9 %	–
RC20*	25149.1	−44.6 %	17.4 %	3043.7	−27.1 %	1.6 %
RC50 + HP	8774.0	−80.7 %	–	1687.9	−59.6 %	–
RC50 + HP*	7304.5	−83.9 %	16.7 %	1659.6	−60.3 %	1.7 %
RC30 + HP	8813.2	−80.6 %	–	1668.6	−60.1 %	–
RC30 + HP*	7304.5	−83.9 %	17.1 %	1659.6	−60.3 %	0.5 %
RC20 + HP	8896.1	−80.4 %	–	1651.7	−60.5 %	–
RC20 + HP*	7304.5	−83.9 %	17.9 %	1659.6	−60.3 %	−0.5 %

Table 12
Generated, exported, self-consumed and delivered electricity comparison among the deep retrofitted analysed scenarios.

Roof insulation + Windows replacement							
Scenario		**RC50***		**RC30***		**RC20***	
		kWh/year		kWh/year		kWh/year	
Electricity consumption	l(t)	24497.6	–	24497.6	–	24485.2	–
Generated Electricity	g(t)	55426.6	226.3 %	43063.4	175.8 %	36863.2	150.6 %
Exported Electricity	e(t)	42080.9	171.8 %	31190.1	127.3 %	25875.6	105.7 %
Delivered Electricity	d(t)	13923.3	56.8 %	14767.5	60.3 %	15340.7	62.7 %
Self-consumed Electricity	s(t)	10574.3	43.2 %	9730.1	39.7 %	9144.5	37.3 %
Net exported Electricity	ne(t)	28157.6	114.9 %	16422.6	67.0 %	10534.9	43.0 %
Scenario		**RC50 + HP***		**RC30 + HP***		**RC20 + HP***	
		kWh/year		kWh/year		kWh/year	
Electricity consumption	l(t)	30337.2	–	30337.2	–	30337.2	–
Generated Electricity	g(t)	55426.6	182.7 %	43063.4	141.9 %	36863.2	121.5 %
Exported Electricity	e(t)	41498.2	136.8 %	30702.7	101.2 %	25440.6	83.9 %
Delivered Electricity	d(t)	19180.3	63.2 %	20125.4	66.3 %	20754.8	68.4 %
Self-consumed Electricity	s(t)	11156.9	36.8 %	10211.8	33.7 %	9582.4	31.6 %
Net exported Electricity	ne(t)	22317.9	73.6 %	10577.4	34.9 %	4685.8	15.4 %

RC50 + HP* scenario, despite the complete electrification, shows a relatively lower but still considerable level of energy generation and export. While the percentage increase in exported energy is relatively minor in all scenarios in comparison to the solutions that solely involve the en-SOLEX system, the results that entail the replacement of the heat generator demonstrate a considerable surge in net exported energy, with percentages ranging from 12.9 % in the RC50 + HP* scenario to 56.8 % in the RC20 + HP* scenario compared to the relative corresponding scenario.

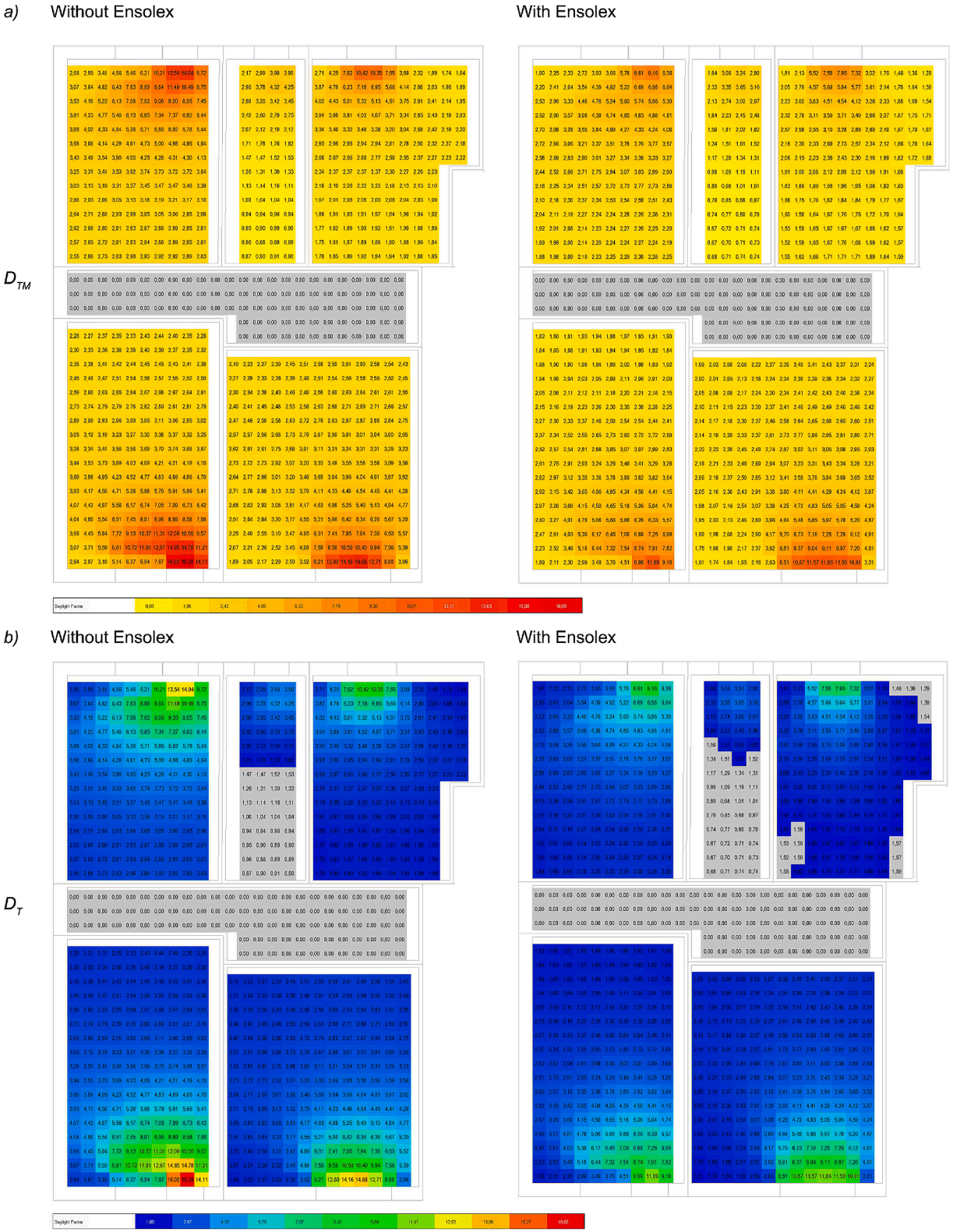

Fig. 17. Minimum Daylight factor (D_{TM}) (a) and Reference Daylight Factor (D_T) (b) consistency analysis with EN 17037 without and without en-SOLEX system.

5.5. Daylight evaluation

Although the shading effect created by the exoskeleton panels proved to be positive in reducing consumption, at the same time this reduces the availability of natural daylight inside the building. A consistency analysis with the daylight limits of EN 17037 [88] (Fig. 17), reveals that, while the minimum daylight factor (D_{TM}) and reference daylight factor (D_T) limits for the analysed location are met for 95 % and 50 % of the floor plane, respectively, when the system is applied, a reduction in the average daylight factor is observed. This reduction ranges from 11 % in the living room to 29 % in the master bedroom (Table 13).

This indicates a generally sufficient provision of natural daylight when the system is implemented. However, the reduction in the average daylight factor, suggests a trade-off between achieving the specified minimum daylight levels and maintaining overall daylight uniformity. Thus, this aspect should be carefully evaluated case by case according to the windows' surface and the room depth of the specific existing building.

5.6. Cost-effectiveness analysis

Since the cost implications of incorporating steel exoskeletons into building projects can be a barrier to widespread adoption, a thorough cost-benefit analysis to justify the investment is needed. To evaluate the cost-effectiveness of the different strategies, the simple payback period (PBP) was calculated by comparing the initial investment cost with the total energy savings achieved by each solution relative to the base case. Additionally, the payback period was assessed considering state incentives for energy retrofitting of existing buildings, which offer a 50 % reduction in the projected investment cost for multi-family building energy retrofitting actions such as heat generator replacement with heat pump, insulation addition over 25 % of scattering surfaces, implementation of shading systems and RES integration.

To estimate the potential economic benefits arising from the implementation of the en-SOLEX system, the saved energy thanks to the system application compared to the baseline scenario was multiplied by the respective average unit costs of 0.244 €/kWh for electricity and 0.11 €/kWh for natural gas, plus the energy savings from self-consumed electricity and the revenue generated from electricity exported to the grid were considered. The calculation of energy savings was based on the reduction in electricity demand from the grid due to self-consumption, which was multiplied by the corresponding average unit cost of 0.244 €/kWh for grid-delivered electricity. Similarly, the surplus electricity exported to the grid was valued at the respective energy price of 0.16 €/kWh paid by the energy supplier [5]. For the evaluation of investment costs, specific unit prices were applied, encompassing both material and installation expenses. The cost for the exoskeleton steel frame, including additional insulation, was set at 350 €/m^2. The En-PV modules were valued at 120 €/module, while the En-Opaque and En-glass modules were priced at 50 €/module. An overall cost of 60,000 € was set for the replacement of heat generator with heat pump and the replacement of all terminal units in the building.

The analysis presented in Table 14 shows that the system integration is associated with significant costs, as evidenced by the extended payback period, which ranges from a maximum of 36.7 years to a minimum of 26.5 years. In particular, interventions that include generator replacement, although initially more expensive, result in a shorter payback period compared to solutions that do not include generator replacement. A critical observation from the analysis is that as the percentage of RES integrated into the exoskeleton system increases, the payback period decreases accordingly. This finding highlights the importance of RES integration in improving the cost-effectiveness of the intervention, as it leads to more favourable results in the cost-benefit analysis. Therefore, solutions that include a higher quota of RES integration are more advantageous in terms of financial returns.

In addition, the payback period improves significantly when considering the impact of government incentives to support energy efficiency improvements in buildings. These incentives significantly improve the economic viability of the intervention, reducing the payback period to a more acceptable level. Specifically, under the influence of government incentives, the payback period ranges from a minimum of 13.2 years in the RC50 + HP scenario to a maximum of 18.3 years in the RC20 scenario. This demonstrates the potential role of policy interventions in accelerating the payback and making such projects more economically viable.

6. Discussion

This study introduces an innovative multifunctional solar exoskeleton as an energy retrofitting solution aimed at maximizing the integration of RES and enhancing on-site energy production in existing buildings, ultimately achieving a net-positive energy goal. The research highlights that, compared to other existing exoskeleton systems, the en-SOLEX system significantly surpasses energy demands in existing buildings, achieving up to 173 % of energy demand coverage based on the total electrification of building energy needs, ensuring a net-positive energy balance in all the scenarios analysed.

In contrast, other systems, such as the diagrid exoskeleton proposed by D'Agostino et al. [18], manage to cover only 47 % of a building's energy consumption. Furthermore, the en-SOLEX system demonstrates superior performance in electricity generation compared to other retrofitting technologies, such as double-skin façades with photovoltaic (PV) integration. For example, the energy retrofitting system studied by Barone et al. [77] can cover up to 95 % of a building's energy demand, which, while effective, does not reach the same level of energy surplus as en-SOLEX.

Nevertheless, the en-SOLEX system presents some limitations. Its application is restricted to buildings with linear profiles and regular structural grids, which reduces its feasibility in more complex architectural forms. Additionally, the presence of balconies or protruding features on the building façade poses challenges to integration, as these elements would need to be removed for successful installation. Moreover, the system requires approximately up to three meters of ground space on each side of the building for proper implementation depending on building height, a condition that is particularly difficult to meet in densely urbanized areas where space is often limited.

While the en-SOLEX system offers substantial benefits in terms of energy efficiency and production, particularly when compared to other existing solutions, its practical application is constrained by

Table 13
Average Daylight factor (DF), minimum daylight factor (D_{TM}) and reference daylight factor (D_T) comparison with and without the en-SOLEX system.

Room	Average Daylight Factor (%)			D_{TM} Fplane% (95 %)			D_T Fplane% (50 %)		
	Without en-Solex	With en-Solex	Δ%	Without en-Solex	With en-Solex	Δ%	Without en-Solex	With en-Solex	Δ%
Master Bedroom	4,5	3,2	−29 %	100 %	100 %	0 %	100 %	100 %	0 %
Kitchen	2,8	2,3	−18 %	100 %	100 %	0 %	100 %	90 %	−10 %
Double Bedroom	4,6	3,3	−27 %	100 %	100 %	0 %	100 %	100 %	0 %
Living Room	3,7	3,3	−11 %	100 %	100 %	0 %	100 %	100 %	0 %

Table 14
Evaluation of the payback period achieved by each scenario.

Investment Cost					Investment Cost with government incentives	Energy saved and exported.	PBP	PBP*
	Steel Frame	En-Modules	HP	Total			year	year
RC50	259,200 €	52,200 €	–	311,400 €	155,700 €	11,244 €	27.7	13.8
RC30	259,200 €	47,160 €	–	306,360 €	153,180 €	9,285 €	33.0	16.5
RC20	259,200 €	44,640 €	–	303,840 €	151,920 €	8,289 €	36.7	18.3
RC50 + HP	259,200 €	52,200 €	60,000 €	371,400 €	185,700 €	14,017 €	26.5	13.2
RC30 + HP	259,200 €	47,160 €	60,000 €	366,360 €	183,180 €	12,057 €	30.4	15.2
RC20 + HP	259,200 €	44,640 €	60,000 €	363,840 €	181,920 €	11,055 €	32.9	16.5

architectural and morphological considerations. This highlights the need for further research and development to increase the flexibility and adaptability of such systems, especially in urban environments where retrofitting opportunities are often limited by space constraints and building design features.

Furthermore, the system was designed with the primary goal of enhancing the energy efficiency of existing buildings, without addressing structural renovation, to offer a more flexible and adaptable solution not depending on the structural behaviour of the existing building. However, in earthquake-prone regions, solely focusing on energy efficiency retrofits without considering seismic retrofit is a limited strategy [51,57,89]. Renovating a building for energy performance alone becomes ineffective if the building remains vulnerable to seismic events, which could potentially damage or destroy the structure, including the newly installed energy-efficient systems. In such contexts, an integrated approach that combines both energy efficiency improvements and seismic reinforcement is not only recommended but essential. A holistic renovation strategy would ensure that buildings are both resilient to seismic hazards and optimized for energy performance. Therefore, future development on the project will investigate the integration of seismic dampers which will connect the structural node of the exoskeleton frame to the structural frame of the existing building to combine energy and seismic upgrades within the retrofitting exoskeleton.

The simulation methodology employed in the paper is subject to certain limitations that should be acknowledged. One of the primary constraints is that the simulation considers the building isolated. While this approach allows for a generalized analysis of the system's energy efficiency, it overlooks potential obstructions caused by neighbouring buildings, which could negatively impact the performance of the PV system by reducing its generation efficiency. Future research should incorporate these external factors to provide a more comprehensive assessment of system performance in realistic urban environments. Furthermore, the current simulations are focused predominantly on evaluating the system's effectiveness in maximizing on-site renewable energy production, particularly through the integration of photovoltaic and shading systems. However, the potential impacts of varying façade configurations – possible through the use of different en-SOLEX system modules –have not been explored in this study. Future investigations could extend this analysis to include the use of greenery panels, bioclimatic greenhouses, and other adaptive shading system technologies.

Another limitation is the use of a fixed façade system in the simulations. For instance, the En-Opaque modules, which provide fixed shading, were shown to be effective in reducing solar radiation during the cooling season while negatively minimizing solar gains during the heating season. Nonetheless, the literature suggests that optimizing façade systems according to specific climatic conditions and building orientations could further enhance the energy efficiency of the system [39,48,90].

It is also important to note that the simulation method evaluated the energy performance of the building at a specific location. However, it is well recognised that the production efficiency of photovoltaics is also dependent on the latitude and average solar irradiation of the site. Thus, changing the building site location could affect the overall results of the system RES generation. To address this issue, Table 15 shows the PV generation achievable by the en-SOLEX system application as the latitude changes according to the main Italian cities.

Based on the analysis, specific recommendations can be provided for the application of the en-SOLEX system to the building's window-to-wall ratio (WWR) and annual energy consumption. For buildings with a WWR of up to 40 %, the RC50 façade configuration is recommended, particularly when energy consumption does not exceed a value of 51,851.3 to 57,134 kWh/year, depending on the site latitude. In cases where the WWR is increased to 60 %, the RC30 façade configuration is recommended, provided that the building's energy consumption remains below a value between 39,075.6 kWh and 43,798 kWh/year. Lastly, for buildings with a WWR of up to 80 %, the RC20 façade configuration is the most suitable, with a maximum energy consumption ranging from 32.675.3 to 37,131 kWh/year.

7. Conclusions

This paper proposes a novel solar exoskeleton for the energy and architectural retrofitting of existing buildings, called "en-SOLEX". The system, which consists of a self-supporting external steel frame, combines passive solar gain control such as shading and greening with high-efficiency active solar systems, including PV panels, optimised for integration into existing building facades. The system aims to increase the surface area available for integrating renewable energy systems in high-density existing buildings. This is crucial as these buildings often have limited space for solar panels, which are typically restricted to the roof surface.

Furthermore, the self-supporting frame of the system enables the panels' load to be directly supported by the structure, thus avoiding additional loads on the existing structure, as they may not able be to withstand additional loads, especially in terms of seismic vulnerability.

The system can be assembled quickly and easily from the outside of the existing building without affecting building occupancy, reducing the time and cost of implementation. The external facade grid's modularity enables easy upgrades and adjustments to the facade modules without compromising the overall system, reducing the environmental impact of retrofitting measures.

The integration of the en-SOLEX system in an existing building was dynamically simulated, demonstrating how the system can reduce energy demand for space heating and cooling by 33.4 % and 25.5 %, respectively. The en-SOLEX system, when combined with generator replacement, can reduce maximum heating and cooling by 80.7 % and 60.5 %, respectively. Furthermore, if combined with deep renovation strategies such as windows replacement and flat roof insulation a higher reduction up to 84 % in heating energy consumption can be achieved.

The integration of RES results in surplus electricity generation, achieving a net positive target for the existing building. The scenarios RC50, RC30, and RC20 exceed the building's electricity demand by 215 %, 170 %, and 150 %, respectively. Meanwhile, scenario RC50 + HP, which fully electrifies building energy needs, even with higher building electricity demand, still generates 165.2 % more electricity than the building requires. Despite fully electrifying building energy needs, the

Table 15
PV generated electricity with the en-SOLEX system according to Italian main cities latitude.

Latitude	Location	RC50		RC30		RC20	
46° 30′ N	Bolzano	53,485.1	kWh/year	39,906.7	kWh/year	33,117.9	kWh/year
45° 28′ N	Milano	52,111.7	kWh/year	39,154.2	kWh/year	32,675.3	kWh/year
44° 30′ N	Bologna	51,851.3	kWh/year	39,075.6	kWh/year	32,687.2	kWh/year
43° 46′ N	Firenze	52,284.5	kWh/year	39,491.1	kWh/year	33,094.8	kWh/year
41° 54′ N	Roma	56,629.3	kWh/year	42,834.3	kWh/year	35,955.2	kWh/year
41° 07′ N	Bari	55,426.5	kWh/year	43,063.4	kWh/year	36,863.3	kWh/year
38° 06′ N	Palermo	57,134.2	kWh/year	43,798.1	kWh/year	37,131.6	kWh/year

net balance remains positive, ranging from 65.2 % with scenario RC50 + HP to 9.9 % with scenario RC20 + HP, turning the retrofitted building into a net energy producer. The surplus electricity exported to the grid allows the retrofitted buildings to provide surplus energy at the district level helping the energy transition of existing urban clusters.

By analysing the system's impact on indoor comfort, it is evident that, while the en-SOLEX system results in a reduction in natural light within the building – albeit within the regulatory limits – it substantially mitigates the hours of thermal discomfort. In particular, a reduction in discomfort hours ranging from 23 to 38 % was observed when comparing the baseline scenario to the retrofitted one.

Even when optimal solar alignment is not feasible due to the varying orientation of existing buildings, the en-SOLEX system demonstrates the ability to achieve a surplus in building energy consumption and meet the net positive energy target. Compared to the south-facing orientation, the east-facing orientation exhibits the greatest reduction in electricity generation, with decreases ranging from 11.8 % in the RC20 + HP scenario to 19.2 % in the RC50 scenario. Although the on-site energy generation is reduced due to the suboptimal orientations, all scenarios ensure a positive net energy balance.

The study's findings indicate that the implementation of the system incurs a significant financial burden when subjected to a cost-benefit analysis under standard economic conditions. The payback period for the intervention ranges from a maximum of 36.7 years to a minimum of 26.5 years. However, the economic feasibility improves significantly when accounting for government incentives designed to promote energy efficiency in buildings. Specifically, the payback period decreases to a range of 13.2 years in the RC50 + HP scenario and as low as 18.3 year in the RC20 scenario. This underscores the critical role of policy measures in expediting the return on investment and enhancing the economic attractiveness of such projects.

The prospective evolution of the system will examine the impact of additional façade configuration modules, including greenery and a bioclimatic greenhouse, on the energy performance of a retrofitted building utilising the en-SOLEX system. Furthermore, an optimisation of the façade modules of the exoskeleton based on building orientation and climatic conditions will be conducted to maximise energy savings and thermal comfort within the building. Additionally, a structural load analysis will be performed to enable the system to provide both energy and structural retrofitting measures simultaneously.

CRediT authorship contribution statement

Roberto Stasi: Writing – review & editing, Writing – original draft, Validation, Software, Methodology, Formal analysis, Conceptualization. **Francesco Ruggiero:** Writing – review & editing, Supervision, Funding acquisition. **Umberto Berardi:** Writing – review & editing, Supervision.

Declaration of competing interest

The authors declare the following financial interests/personal relationships which may be considered as potential competing interests: Francesco Ruggiero reports financial support was provided by Sud Montaggi S.r.L. If there are other authors, they declare that they have no known competing financial interests or personal relationships that could have appeared to influence the work reported in this paper.

Acknowledgements

The authors acknowledge the financial support provided by Regione Puglia (Italy) for the project named "En-SOLEX - Esoscheletri ad energia solare per la riqualificazione degli edifici" within the financial frame "RIPARTI-assegni di Ricerca per riPARTire con le Imprese". This research was conducted within the frame of the research agreement "*ReNew Urban- esoscheletri per la riqualificazione energetica e sismica di edifici esistenti"* between Sud Montaggi S.r.l. company and Department of Civil Architecture, Built Environment and Design of Polytechnic University of Bari.

The authors recognize the financial contribution of the following projects: PRIN - HERA – "Holistic Energy Recovery Agent tool for sustainable urban clusters" and PRIN PNRR 2022 NETPLUS – "Neighborhood Energy Transition: towards Positive energy baLance and carbon neUtral diStricts".

Appendix 1

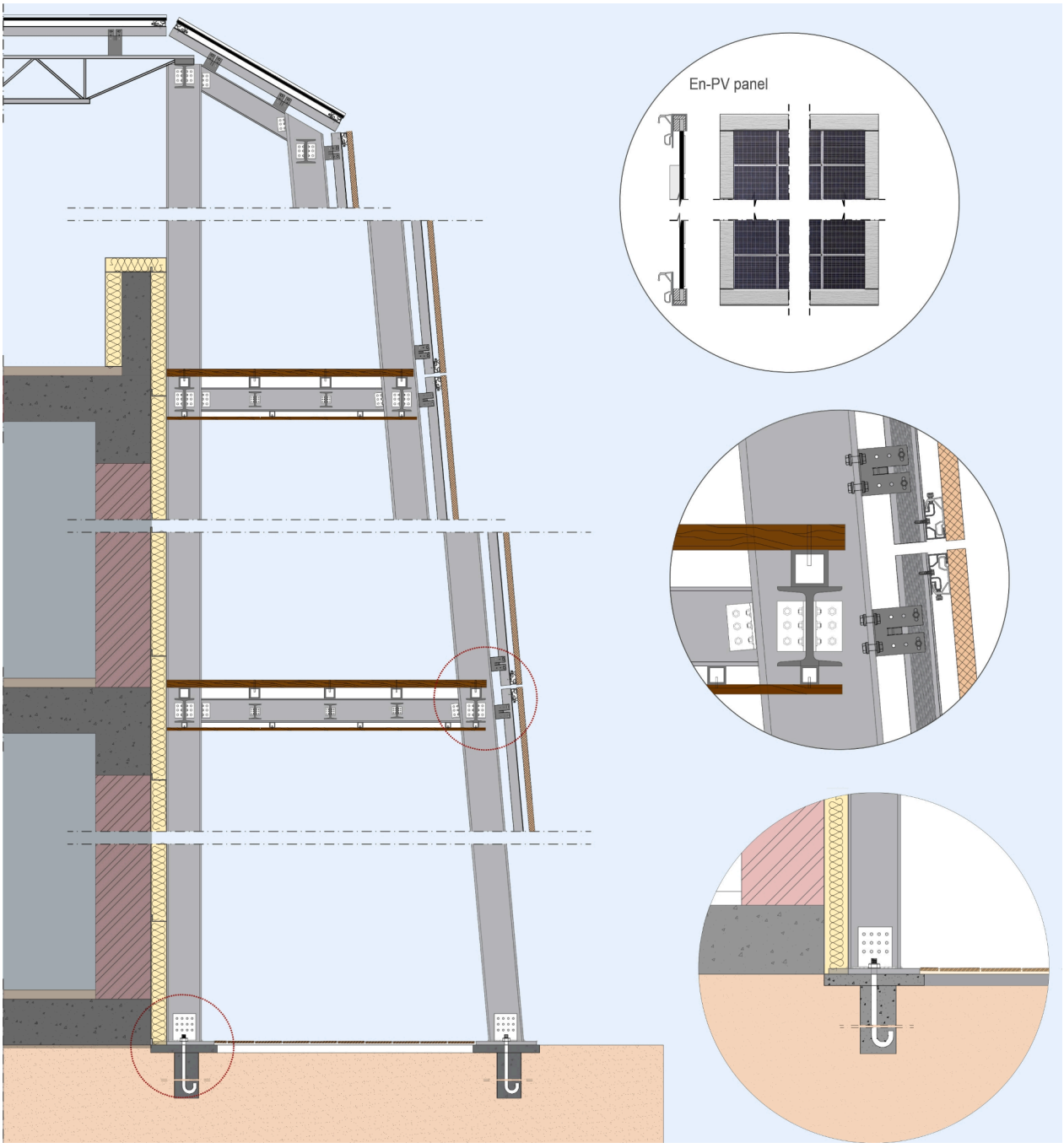

Fig. 18. Technical detail drawing of the en-SOLEX system.

Appendix 2

Table 16
Generated, exported, self-consumed and delivered electricity comparison among the analysed scenarios based on different building orientations.

East							
Scenario		**RC50**	**RC30**	**RC20**	**RC50 + HP**	**RC30 + HP**	**RC20 + HP**
		kWh/ year	kWh/ year	kWh/ year	kWh/ year	kWh/ year	kWh/ year

(*continued on next page*)

Table 16 (*continued*)

East													
Scenario		**RC50**		**RC30**		**RC20**		**RC50 + HP**		**RC30 + HP**		**RC20 + HP**	
		kWh/ year		kWh/ year		kWh/ year		kWh/ year		kWh/ year		kWh/ year	
Electrity consumption	l(t)	26106.1	–	26066.4	–	26060.7	–	33022.6	–	33022.6	–	33022.6	–
Generated Electricity	g(t)	47521.6	182.0 %	38304.9	147.0 %	33681.9	129.2 %	47521.6	143.9 %	38304.9	116.0 %	33681.9	102.0 %
Exported Electricity	e(t)	32,803	125.7 %	25,026	96.0 %	21454.6	82.3 %	32499.2	98.4 %	24756.9	75.0 %	21162.7	64.1 %
Delivered Electricity	d(t)	13763.6	52.7 %	14702.8	56.4 %	15517.5	59.5 %	20376.3	61.7 %	21389.8	64.8 %	22187.5	67.2 %
Self-consumed Electricity	s(t)	12342.5	47.3 %	11363.6	43.6 %	10543.2	40.5 %	12646.3	38.3 %	11632.8	35.2 %	10835.1	32.8 %
Net exported Electricity	ne (t)	19039.4	72.9 %	10323.3	39.6 %	5937.1	22.8 %	12122.8	36.7 %	3369.7	10.2 %	1022.7	3.1 %
South-East													
Scenario		**RC50** kWh/ year		**RC30** kWh/ year		**RC20** kWh/ year		**RC50 + HP** kWh/ year		**RC30 + HP** kWh/ year		**RC20 + HP** kWh/ year	
Electrity consumption	l(t)	25015.4	–	24996.9	–	24990.5	–	32264.8	–	32264.8	–	32264.8	–
Generated Electricity	g(t)	53498.6	213.9 %	41903.8	167.6 %	36,088	144.4 %	53498.6	165.8 %	41903.8	129.9 %	36,088	111.8 %
Exported Electricity	e(t)	39051.3	156.1 %	28965.7	115.9 %	24194.6	96.8 %	38481.9	119.3 %	28488.6	88.3 %	23754.1	73.6 %
Delivered Electricity	d(t)	13243.1	52.9 %	14,154	56.6 %	14901.5	59.6 %	19923.1	61.7 %	20944.8	64.9 %	21735.3	67.4 %
Self-consumed Electricity	s(t)	11772.3	47.1 %	10842.9	43.4 %	10,089	40.4 %	12341.7	38.3 %	11,320	35.1 %	10529.5	32.6 %
Net exported Electricity	ne (t)	25808.2	103.2 %	14811.7	59.3 %	9293	37.2 %	18558.7	57.5 %	7547.4	23.4 %	2021.8	6.3 %
South													
Scenario		RC50 kWh/ year		RC30 kWh/ year		RC20 kWh/ year		RC50 + HP kWh/ year		RC30 + HP kWh/ year		RC20 + HP kWh/ year	
Electrity consumption	l(t)	24594.8	–	24584.6	–	24581.9	–	31882.5	–	31882.5	–	31882.5	–
Generated Electricity	g(t)	55426.5	225.4 %	43063.4	175.2 %	36863.3	150.0 %	55426.5	173.8 %	43063.4	135.1 %	36863.3	115.6 %
Exported Electricity	e(t)	42033.7	170.9 %	31114.2	126.6 %	25831.1	105.1 %	41321.0	129.6 %	30555.8	95.8 %	25306.3	79.4 %
Delivered Electricity	d(t)	13973.3	56.8 %	14818.6	60.3 %	15392.9	62.6 %	20548.3	64.5 %	21523.0	67.5 %	22165.8	69.5 %
Self-consumed Electricity	s(t)	10621.5	43.2 %	9766.0	39.7 %	9189.0	37.4 %	11334.2	35.5 %	10359.5	32.5 %	9716.8	30.5 %
Net exported Electricity	ne (t)	28060.4	114.1 %	16295.6	66.3 %	10438.2	42.5 %	20772.7	65.2 %	9032.8	28.3 %	3140.6	9.9 %
South West													
Scenario		**RC50** kWh/ year		**RC30** kWh/ year		**RC20** kWh/ year		**RC50 + HP** kWh/ year		**RC30 + HP** kWh/ year		**RC20 + HP** kWh/ year	
Electrity consumption	l(t)	25027.2	–	24998.2	–	24992.4	–	32263.1	–	32263.1	–	32263.1	–
Generated Electricity	g(t)	53507.3	213.8 %	41,909	167.6 %	36,092	144.4 %	53507.3	165.8 %	41,909	129.9 %	36,092	111.9 %
Exported Electricity	e(t)	40646.6	162.4 %	30449.2	121.8 %	25425.6	101.7 %	40102.1	124.3 %	29924.7	92.8 %	24912.3	77.2 %
Delivered Electricity	d(t)	14841.9	59.3 %	15633.8	62.5 %	16130.6	64.5 %	21533.3	66.7 %	22374.2	69.3 %	22,888	70.9 %
Self-consumed Electricity	s(t)	10185.3	40.7 %	9364.4	37.5 %	8861.8	35.5 %	10729.8	33.3 %	9888.9	30.7 %	9375.1	29.1 %
Net exported Electricity	ne (t)	25804.7	103.1 %	14815.3	59.3 %	9294.9	37.2 %	18568.7	57.6 %	7554.1	23.4 %	2026.9	6.3 %
West													
Scenario		**RC50** kWh/ year		**RC30** kWh/ year		**RC20** kWh/ year		**RC50 + HP** kWh/ year		**RC30 + HP** kWh/ year		**RC20 + HP** kWh/ year	
Electrity consumption	l(t)	26002.5	–	25994.2	–	25988.9	–	32993.1	–	32993.1	–	32993.1	–
Generated Electricity	g(t)	47512.6	182.7 %	38298.4	147.3 %	33677.5	129.6 %	47512.6	144.0 %	38298.4	116.1 %	33677.5	102.1 %
Exported Electricity	e(t)	34516.7	132.7 %	26615.7	102.4 %	22,753	87.5 %	34170.6	103.6 %	26257.8	79.6 %	22382.3	67.8 %
Delivered Electricity	d(t)	15402.3	59.2 %	16226.4	62.4 %	16748.3	64.4 %	22026.8	66.8 %	22867.4	69.3 %	23381.8	70.9 %
Self-consumed Electricity	s(t)	10600.2	40.8 %	9767.8	37.6 %	9240.6	35.6 %	10966.3	33.2 %	10125.7	30.7 %	9611.3	29.1 %
Net exported Electricity	ne (t)	19114.4	73.5 %	10389.3	40.0 %	6004.7	23.1 %	12143.8	36.8 %	3390.4	10.3 %	999.5	3.0 %

Data availability

Data will be made available on request.

References

[1] European Commission, COM/2019/640 final - The European Green Deal., (2019).
[2] C. Maduta, G. Melica, D. D'Agostino, P. Bertoldi, Towards a decarbonised building stock by 2050: the meaning and the role of zero emission buildings (ZEBs) in Europe, Energ. Strat. Rev. 44 (2022) 101009, https://doi.org/10.1016/J.ESR.2022.101009.
[3] J. Dolšak, Determinants of energy efficient retrofits in residential sector: a comprehensive analysis, Energ. Buildings 282 (2023) 112801, https://doi.org/10.1016/J.ENBUILD.2023.112801.
[4] Perspectives for the Clean Energy Transition – Analysis - IEA, 2019. https://www.iea.org/reports/the-critical-role-of-buildings.
[5] Eurostat, Eurostat Statistics Explained, 2024. https://ec.europa.eu/eurostat/statistics-explained/index.php?title=Electricity_price_statistics#cite_note-1.
[6] M. Economidou, V. Todeschi, P. Bertoldi, D. D'agostino, P. Zangheri, L. Castellazzi, Review of 50 years of EU energy efficiency policies for buildings, (2020). 10.1016/j.enbuild.2020.110322.
[7] U. Berardi, ZEB and NZEB (definitions, design methodologies, good practices, and case studies), Handbook of Energy Efficiency in Buildings: A Life Cycle Approach (2018), https://doi.org/10.1016/B978-0-12-812817-6.00038-3.
[8] D. D'Agostino, L. Mazzarella, Data on energy consumption and Nearly zero energy buildings (NZEBs) in Europe, Data Brief 21 (2018) 2470–2474, https://doi.org/10.1016/j.dib.2018.11.094.
[9] European Commission, Directive (EU) 2018/844, Official Journal of the European Union (2018).
[10] R. Landolfo, A. Formisano, G. Di Lorenzo, A. Di Filippo, Classification of european building stock in technological and typological classes, Journal of Building Engineering 45 (2022) 103482, https://doi.org/10.1016/J.JOBE.2021.103482.
[11] Istat, Data warehouse del censimento della popolazione e delle abitazioni italiane, Annuario Statistico Italiano (2018).
[12] F. Ascione, R.F. De Masi, M. Mastellone, S. Ruggiero, G.P. Vanoli, Improving the building stock sustainability in European Countries: a focus on the Italian case, J. Clean. Prod. 365 (2022) 132699, https://doi.org/10.1016/J.JCLEPRO.2022.132699.
[13] European Commission, 'The European Green Deal', Brussels, Belgium, 2019.
[14] R. Stasi, F. Ruggiero, U. Berardi, Evaluation of mixed mode ventilation cooling energy saving potential in nZEB: A case study in Southern Italy, E3S Web of Conferences 343 (2022) 01004, https://doi.org/10.1051/E3SCONF/202234301004.
[15] F. Pacheco-Torgal, Introduction to cost-effective energy-efficient building retrofitting, cost-effective energy efficient building retrofitting: materials, technologies, Optimization and Case Studies (2017) 1–20, https://doi.org/10.1016/B978-0-08-101128-7.00001-0.
[16] W. Ahmed, M. Asif, A critical review of energy retrofitting trends in residential buildings with particular focus on the GCC countries, Renew. Sustain. Energy Rev. 144 (2021) 111000, https://doi.org/10.1016/J.RSER.2021.111000.
[17] J.A. Dauda, S.O. Ajayi, Understanding the impediments to sustainable structural retrofit of existing buildings in the UK, Journal of Building Engineering 60 (2022) 105168, https://doi.org/10.1016/J.JOBE.2022.105168.
[18] D. D'Agostino, D. Faiella, E. Febbraro, E. Mele, F. Minichiello, J. Trimarco, Steel exoskeletons for integrated seismic/energy retrofit of existing buildings - general framework and case study, Journal of Building Engineering 83 (2024) 108413, https://doi.org/10.1016/J.JOBE.2023.108413.
[19] F. Ascione, N. Bianco, G.M. Mauro, D.F. Napolitano, Retrofit of villas on Mediterranean coastlines: pareto optimization with a view to energy-efficiency and cost-effectiveness, Appl. Energy 254 (2019) 113705, https://doi.org/10.1016/j.apenergy.2019.113705.
[20] N.S. Ibañez Iralde, J. Pascual, J. Salom, Energy retrofit of residential building clusters. a literature review of crossover recommended measures, policies instruments and allocated funds in Spain, Energy Build 252 (2021) 111409, https://doi.org/10.1016/J.ENBUILD.2021.111409.
[21] C. Citadini de Oliveira, I. Catão Martins Vaz, E. Ghisi, Retrofit strategies to improve energy efficiency in buildings: an integrative review, Energy Build 321 (2024) 114624. 10.1016/J.ENBUILD.2024.114624.
[22] M. Ibrahim, F. Harkouss, P. Biwole, F. Fardoun, S. Ouldboukhitine, Building retrofitting towards net zero energy: a review, Energ. Buildings 322 (2024) 114707, https://doi.org/10.1016/J.ENBUILD.2024.114707.
[23] B. Abu-Jdayil, A.H. Mourad, W. Hittini, M. Hassan, S. Hameedi, Traditional, state-of-the-art and renewable thermal building insulation materials: an overview, Constr. Build. Mater. 214 (2019) 709–735, https://doi.org/10.1016/J.CONBUILDMAT.2019.04.102.
[24] R. Suárez, J. Fernández-Agüera, Passive energy strategies in the retrofitting of the residential sector: a practical case study in dry hot climate, Build. Simul. 8 (2015) 593–602, https://doi.org/10.1007/S12273-015-0234-7.
[25] B. Ozarisoy, H. Altan, Handbook of retrofitting high density residential buildings: policy design and implications on domestic energy use in the eastern mediterranean climate of cyprus, Handbook of Retrofitting High Density Residential Buildings: Policy Design and Implications on Domestic Energy Use in the Eastern Mediterranean Climate of Cyprus (2023) 1–864, https://doi.org/10.1007/978-3-031-11854-8/COVER.
[26] A.A. Chowdhury, M.G. Rasul, M.M.K. Khan, Thermal performance assessment of a retrofitted building using an integrated energy and computational fluid dynamics (IE - CFD) approach, Energy Rep. 8 (2022) 709–717, https://doi.org/10.1016/J.EGYR.2022.10.365.
[27] S. Schiavoni, F. D'Alessandro, F. Bianchi, F. Asdrubali, Insulation materials for the building sector: a review and comparative analysis, Renew. Sustain. Energy Rev. 62 (2016) 988–1011, https://doi.org/10.1016/J.RSER.2016.05.045.
[28] R. Tällberg, B.P. Jelle, R. Loonen, T. Gao, M. Hamdy, Comparison of the energy saving potential of adaptive and controllable smart windows: a state-of-the-art review and simulation studies of thermochromic, photochromic and electrochromic technologies, Sol. Energy Mater. Sol. Cells 200 (2019) 109828, https://doi.org/10.1016/J.SOLMAT.2019.02.041.
[29] Z. Zhou, C. Wang, X. Sun, F. Gao, W. Feng, G. Zillante, Heating energy saving potential from building envelope design and operation optimization in residential buildings: a case study in northern China, J. Clean. Prod. 174 (2018) 413–423, https://doi.org/10.1016/J.JCLEPRO.2017.10.237.
[30] R. Stasi, F. Ruggiero, U. Berardi, Assessing the Potential of Phase-Change Materials in Energy Retrofitting of Existing Buildings in a Mediterranean Climate, Energies 2024, Vol. 17, Page 4839 17 (2024) 4839. 10.3390/EN17194839.
[31] S. Dardouri, S. Mankai, M.M. Almoneef, M. Mbarek, J. Sghaier, Energy performance based optimization of building envelope containing PCM combined with insulation considering various configurations, Energy Rep. 10 (2023) 895–909, https://doi.org/10.1016/J.EGYR.2023.07.050.
[32] U.Y. Ayikoe Tettey, L. Gustavsson, Energy savings and overheating risk of deep energy renovation of a multi-storey residential building in a cold climate under climate change, Energy 202 (2020) 117578, https://doi.org/10.1016/J.ENERGY.2020.117578.
[33] Y. Chen, J. Gao, J. Yang, U. Berardi, G. Cui, An hour-ahead predictive control strategy for maximizing natural ventilation in passive buildings based on weather forecasting, Appl. Energy 333 (2023) 120613. ISSN 0306-2619, https://doi.org/10.1016/j.apenergy.2022.120613.
[34] R. Stasi, F. Ruggiero, U. Berardi, The efficiency of hybrid ventilation on cooling energy savings in NZEBs, Journal of Building Engineering 53 (2022) 104401, https://doi.org/10.1016/j.jobe.2022.104401.
[35] C. Li, Y. Chen, A multi-factor optimization method based on thermal comfort for building energy performance with natural ventilation, Energ. Buildings 285 (2023) 112893, https://doi.org/10.1016/J.ENBUILD.2023.112893.
[36] C.M. Calama-González, R. Escandón, A. Alonso, R. Suárez, Á.L. León-Rodríguez, A. Sánchez-Ostiz Gutiérrez, A. Arriazu-Ramos, A. Monge-Barrio, Thermal insulation impact on overheating vulnerability reduction in Mediterranean dwellings, Heliyon 9 (2023) e16102, https://doi.org/10.1016/J.HELIYON.2023.E16102.
[37] R. Stasi, F. Ruggiero, U. Berardi, Natural ventilation effectiveness in low-income housing to challenge energy poverty, Energ. Buildings 304 (2024) 113836, https://doi.org/10.1016/J.ENBUILD.2023.113836.
[38] H. Wu, T. Zhang, Optimal design of complex dynamic shadings: towards sustainable built environment, Sustain. Cities Soc. 86 (2022) 104109, https://doi.org/10.1016/J.SCS.2022.104109.
[39] A. Tabadkani, A. Roetzel, H.X. Li, A. Tsangrassoulis, Design approaches and typologies of adaptive facades: a review, Autom. Constr. 121 (2021) 103450, https://doi.org/10.1016/J.AUTCON.2020.103450.
[40] A. Ibrahim, M. Alsukkar, Y. Dong, P. Hu, Improvements in energy savings and daylighting using trapezoid profile louver shading devices, Energ. Buildings 321 (2024) 114649, https://doi.org/10.1016/J.ENBUILD.2024.114649.
[41] B. Ghaleb, M. Asif, Application of solar PV in commercial buildings: Utilizability of rooftops, Energ. Buildings 257 (2022) 111774, https://doi.org/10.1016/J.ENBUILD.2021.111774.
[42] M. Alhuyi Nazari, J. Rungamornrat, L. Prokop, V. Blazek, S. Misak, M. Al-Bahrani, M.H. Ahmadi, An updated review on integration of solar photovoltaic modules and heat pumps towards decarbonization of buildings, Energy Sustain. Dev. 72 (2023) 230–242, https://doi.org/10.1016/J.ESD.2022.12.018.
[43] Z. Zhu, Y. Wang, M. Yuan, R. Zhang, Y. Chen, G. Lou, Y. Sun, Energy saving and carbon reduction schemes for families with the household PV-BES-EV system, Energ. Buildings 288 (2023) 113007, https://doi.org/10.1016/J.ENBUILD.2023.113007.
[44] I. Ballarini, V. Corrado, F. Madonna, S. Paduos, F. Ravasio, Energy refurbishment of the Italian residential building stock: energy and cost analysis through the application of the building typology, Energy Policy 105 (2017) 148–160, https://doi.org/10.1016/j.enpol.2017.02.026.
[45] F. Calise, F.L. Cappiello, L. Cimmino, M. Dentice d'Accadia, M. Vicidomini, Dynamic modelling and thermoeconomic analysis for the energy refurbishment of the Italian building sector: Case study for the "Superbonus 110 %" funding strategy, Appl Therm Eng 213 (2022) 118689. 10.1016/J.APPLTHERMALENG.2022.118689.
[46] W.T. Wang, H. Yang, C.Y. Xiang, Green roofs and facades with integrated photovoltaic system for zero energy eco-friendly building – a review, Sustainable Energy Technol. Assess. 60 (2023) 103426, https://doi.org/10.1016/J.SETA.2023.103426.

[47] W. Zou, Y. Wang, E. Tian, J. Wei, J. Peng, J. Mo, A new dynamic and vertical photovoltaic integrated building envelope for high-rise glaze-facade buildings, Engineering (2024), https://doi.org/10.1016/J.ENG.2024.01.014.
[48] P. Jayathissa, M. Luzzatto, J. Schmidli, J. Hofer, Z. Nagy, A. Schlueter, Optimising building net energy demand with dynamic BIPV shading, Appl. Energy 202 (2017) 726–735, https://doi.org/10.1016/J.APENERGY.2017.05.083.
[49] C. Xiang, B.S. Matusiak, Façade Integrated Photovoltaics design for high-rise buildings with balconies, balancing daylight, aesthetic and energy productivity performance, Journal of Building Engineering 57 (2022) 104950, https://doi.org/10.1016/J.JOBE.2022.104950.
[50] M.V. Requena-Garcia-Cruz, J. Díaz-Borrego, E. Romero-Sánchez, A. Morales-Esteban, M.A. Campano, Assessment of integrated solutions for the combined energy efficiency improvement and seismic strengthening of existing URM buildings, Buildings 2022, Vol. 12, Page 1276 12 (2022) 1276. 10.3390/BUILDINGS12081276.
[51] C. Menna, C. Del Vecchio, M. Di Ludovico, G.M. Mauro, F. Ascione, A. Prota, Conceptual design of integrated seismic and energy retrofit interventions, Journal of Building Engineering (2021) 102190, https://doi.org/10.1016/j.jobe.2021.102190.
[52] G. Evola, V. Costanzo, A. Urso, C. Tardo, G. Margani, Energy performance of a prefabricated timber-based retrofit solution applied to a pilot building in Southern Europe, Build. Environ. 222 (2022) 109442, https://doi.org/10.1016/J.BUILDENV.2022.109442.
[53] G. Santarsiero, A. D'Angola, G. Ventura, A. Masi, V. Manfredi, V. Picciano, A. Digrisolo, Sustainable renovation of public buildings through seismic–energy upgrading: methodology and application to an RC school building, Infrastructures 2023, Vol. 8, Page 168 8 (2023) 168. 10.3390/INFRASTRUCTURES8120168.
[54] G. Aruta, F. Ascione, N. Bianco, T. Iovane, G.M. Mauro, A responsive double-skin façade for the retrofit of existing buildings: analysis on an office building in a Mediterranean climate, Energ. Buildings 284 (2023) 112850, https://doi.org/10.1016/J.ENBUILD.2023.112850.
[55] D.A. Pohoryles, D.A. Bournas, F. Da Porto, A. Caprino, G. Santarsiero, T. Triantafillou, Integrated seismic and energy retrofitting of existing buildings: a state-of-the-art review, Journal of Building Engineering 61 (2022) 105274, https://doi.org/10.1016/J.JOBE.2022.105274.
[56] S. Labò, C. Passoni, A. Marini, A. Belleri, Design of diagrid exoskeletons for the retrofit of existing RC buildings, Eng. Struct. 220 (2020) 110899, https://doi.org/10.1016/J.ENGSTRUCT.2020.110899.
[57] L. Martelli, L. Restuccia, G.A. Ferro, The exoskeleton: a solution for seismic retrofitting of existing buildings, Procedia Struct. Integrity 25 (2020) 294–304, https://doi.org/10.1016/J.PROSTR.2020.04.034.
[58] D. Foti, F. Ruggiero, M.F. Sabbà, M. Lerna, A dissipating frames for seismic retrofitting and building energy-efficiency, Infrastructures 2020, Vol. 5, Page 74 5 (2020) 74. 10.3390/INFRASTRUCTURES5090074.
[59] J. Olivo, R. Cucuzza, G. Bertagnoli, M. Domaneschi, Optimal design of steel exoskeleton for the retrofitting of RC buildings via genetic algorithm, Comput. Struct. 299 (2024) 107396, https://doi.org/10.1016/J.COMPSTRUC.2024.107396.
[60] R.E. Weber, C. Mueller, C. Reinhart, Solar exoskeletons – an integrated building system combining solar gain control with structural efficiency, Sol. Energy 240 (2022) 301–314, https://doi.org/10.1016/J.SOLENER.2022.05.048.
[61] L.F. Cabeza, L. Boquera, M. Chàfer, D. Vérez, Embodied energy and embodied carbon of structural building materials: worldwide progress and barriers through literature map analysis, Energ. Buildings 231 (2021) 110612, https://doi.org/10.1016/J.ENBUILD.2020.110612.
[62] A. Marini, C. Passoni, A. Belleri, F. Feroldi, M. Preti, G. Metelli, P. Riva, E. Giuriani, G. Plizzari, Combining seismic retrofit with energy refurbishment for the sustainable renovation of RC buildings: a proof of concept, Eur. J. Environ. Civ. Eng. 26 (2022) 2475–2495, https://doi.org/10.1080/19648189.2017.1363665.
[63] F. Morris, S. Allen, W. Hawkins, On the embodied carbon of structural timber versus steel, and the influence of LCA methodology, Build. Environ. 206 (2021) 108285, https://doi.org/10.1016/J.BUILDENV.2021.108285.
[64] W. Hawkins, S. Cooper, S. Allen, J. Roynon, T. Ibell, Embodied carbon assessment using a dynamic climate model: case-study comparison of a concrete, steel and timber building structure, Structures 33 (2021) 90–98, https://doi.org/10.1016/J.ISTRUC.2020.12.013.
[65] O.E. Bellini, A. Marini, C. Passoni, Adaptive exoskeleton systems for the resilience of the built environment, TECHNE - Journal of Technology for Architecture and Environment 15 (2018) 71–80. 10.13128/TECHNE-22120.
[66] A. Ferrante, G. Mochi, G. Predari, L. Badini, A. Fotopoulou, R. Gulli, G. Semprini, A European Project for Safer and Energy Efficient Buildings: Pro-GET-onE (Proactive Synergy of inteGrated Efficient Technologies on Buildings' Envelopes), Sustainability 2018, Vol. 10, Page 812 10 (2018) 812. 10.3390/SU10030812.
[67] S. D'Urso, B. Cicero, From the efficiency of nature to parametric design. A holistic approach for sustainable building renovation in seismic regions, Sustainability 2019, Vol. 11, Page 1227 11 (2019) 1227. 10.3390/SU11051227.
[68] A. Bruck, S. Diaz Ruano, H. Auer, Values and implications of building envelope retrofitting for residential positive energy districts, Energy Build 275 (2022) 112493, https://doi.org/10.1016/J.ENBUILD.2022.112493.
[69] H. Du, Q. Han, B. de Vries, J. Sun, Community solar PV adoption in residential apartment buildings: a case study on influencing factors and incentive measures in Wuhan, Appl. Energy 354 (2024) 122163, https://doi.org/10.1016/J.APENERGY.2023.122163.
[70] J.R.C.I. for the P. and S. of the Citizen, M. Economidou, P. Bertoldi, Financing building energy renovations – Current experiences and ways forward, Publications Office, 2014. doi/10.2790/28190.
[71] I. Ballarini, S.P. Corgnati, V. Corrado, Use of reference buildings to assess the energy saving potentials of the residential building stock: the experience of TABULA project, Energy Policy 68 (2014) 273–284, https://doi.org/10.1016/J.ENPOL.2014.01.027.
[72] T. Loga, B. Stein, N. Diefenbach, TABULA building typologies in 20 European countries—making energy-related features of residential building stocks comparable, Energ. Buildings 132 (2016) 4–12, https://doi.org/10.1016/J.ENBUILD.2016.06.094.
[73] L. Appolloni, D. D'alessandro, Housing spaces in nine European Countries: a comparison of dimensional requirements, International Journal of Environmental Research and Public Health 2021, Vol. 18, Page 4278 18 (2021) 4278. 10.3390/IJERPH18084278.
[74] C. Baglivo, D. Mazzeo, S. Panico, S. Bonuso, N. Matera, P.M. Congedo, G. Oliveti, Complete greenhouse dynamic simulation tool to assess the crop thermal well-being and energy needs, Appl. Therm. Eng. 179 (2020) 115698, https://doi.org/10.1016/J.APPLTHERMALENG.2020.115698.
[75] G. Hou, X. Zhai, Y. Kuai, P. Shu, P. Zhang, S. Wei, A systematic review on studies of thermal comfort in building transitional space, Journal of Building Engineering 89 (2024) 109280, https://doi.org/10.1016/J.JOBE.2024.109280.
[76] M. Gonçalves, A. Figueiredo, R.M.S.F. Almeida, R. Vicente, Dynamic façades in buildings: a systematic review across thermal comfort, energy efficiency and daylight performance, Renew. Sustain. Energy Rev. 199 (2024) 114474, https://doi.org/10.1016/J.RSER.2024.114474.
[77] G. Barone, I. Vardopoulos, S. Attia, C. Vassiliades, Optimizing energy-efficient building renovation: Integrating double-skin façades with solar systems in the Mediterranean landscape, (2024). 10.1016/j.egyr.2024.08.032.
[78] E. Santolini, B. Pulvirenti, P. Guidorzi, M. Bovo, D. Torreggiani, P. Tassinari, Analysis of the effects of shading screens on the microclimate of greenhouses and glass facade buildings, Build. Environ. 211 (2022) 108691, https://doi.org/10.1016/J.BUILDENV.2021.108691.
[79] F. Asdrubali, F. Cotana, A. Messineo, On the evaluation of solar greenhouse efficiency in building simulation during the heating period, Energies (Basel) 5 (2012) 1864–1880, https://doi.org/10.3390/en5061864.
[80] F. Xue, S.S.Y. Lau, Z. Gou, Y. Song, B. Jiang, Incorporating biophilia into green building rating tools for promoting health and wellbeing, Environ. Impact Assess. Rev. 76 (2019) 98–112, https://doi.org/10.1016/J.EIAR.2019.02.004.
[81] J. Coma, G. Pérez, A. de Gracia, S. Burés, M. Urrestarazu, L.F. Cabeza, Vertical greenery systems for energy savings in buildings: a comparative study between green walls and green facades, Build. Environ. 111 (2017) 228–237, https://doi.org/10.1016/J.BUILDENV.2016.11.014.
[82] W. Che, W. Zhuang, Integrating vertical greenery for complex building patterns towards sustainable urban environment, Sustain. Cities Soc. 113 (2024) 105684, https://doi.org/10.1016/J.SCS.2024.105684.
[83] M. Su, P. Jie, P. Li, F. Yang, Z. Huang, X. Shi, A review on the mechanisms behind thermal effect of building vertical greenery systems (VGS): methodology, performance and impact factors, Energ. Buildings 303 (2024) 113785, https://doi.org/10.1016/J.ENBUILD.2023.113785.
[84] D.M. 26/06/2015, Applicazione delle metodologie di calcolo delle prestazioni energetiche e definizione delle prescrizioni e dei requisiti minimi degli edifici, Italy, 2015.
[85] K. Voss, I. Sartori, A. Napolitano, S. Geier, H. Gonzalves, M. Hall, J. Widén, J.A. Candanedo, E. Musall, B. Karlsson, P. Torcellini, Load Matching and Grid Interaction of Net Zero Energy Buildings, (2010).
[86] UNI EN Standard 16798-2, Energy Performance of Buildings—Ventilation for Buildings—Part. 2: Interpretation of the Requirements in EN 16798-1—Indoor Environmental Input Parameters for Design and Assessment of Energy Performance of Buildings Addressing Indoor Air Quality, Thermal E, (2019).
[87] C. Piccardo, L. Gustavsson, Deep energy retrofits using different retrofit materials under different scenarios: life cycle cost and primary energy implications, Energy 281 (2023) 128131, https://doi.org/10.1016/J.ENERGY.2023.128131.
[88] J. Hraška, J. Ćurpek, The practical implications of the EN 17037 minimum target daylight factor for building design and urban daylight in several European countries, Heliyon 10 (2024) e23297, https://doi.org/10.1016/J.HELIYON.2023.E23297.
[89] E. Meglio, G. Longobardi, A. Formisano, Integrated seismic-energy retrofit systems for preventing failure of a historical RC school building: comparison among metal lightweight exoskeleton solutions, Eng. Fail. Anal. 154 (2023) 107663, https://doi.org/10.1016/J.ENGFAILANAL.2023.107663.
[90] S.M. Al-Masrani, K.M. Al-Obaidi, N.A. Zalin, M.I. Aida Isma, Design optimisation of solar shading systems for tropical office buildings: challenges and future trends, Solar Energy 170 (2018) 849–872, https://doi.org/10.1016/J.SOLENER.2018.04.047.